



**FATİH UNIVERSITY**

**The Graduate School of Sciences and Engineering**

**Master of Science in  
Genetics and Bioengineering**

**AMPEROMETRIC BIOSENSOR FOR DETECTION OF  
XANTHINE LEVEL FOR MEAT FRESHNESS  
CONTROL**

**by**

**Muamer DERVISEVIC**

**September 2015**



**AMPEROMETRIC BIOSENSOR FOR DETECTION OF  
XANTHINE LEVEL FOR MEAT FRESHNESS CONTROL**

by

Muamer DERVISEVIC

A thesis submitted to

the Graduate School of Sciences and Engineering

of

Fatih University

in partial fulfillment of the requirements for the degree of

Master of Science

in

Genetics and Bioengineering

September 2015  
Istanbul, Turkey

## APPROVAL PAGE

This is to certify that I have read this thesis written by Muamer DERVISEVIC and that in my opinion it is fully adequate, in scope and quality, as a thesis for the degree of Master of Science in Genetics and Bioengineering.

\_\_\_\_\_  
Assoc. Prof. M. Fatih ABASIYANIK  
Thesis Supervisor

\_\_\_\_\_  
Assoc. Prof. Mehmet ŞENEL  
Co-Supervisor

I certify that this thesis satisfies all the requirements as a thesis for the degree of Master of Science in Genetics and Bioengineering.

\_\_\_\_\_  
Assoc. Prof. M. Fatih ABASIYANIK  
Head of Department

Examining Committee Members

Assoc. Prof. Fatih Mustafa ABASIYANIK \_\_\_\_\_

Assoc. Prof. Kurtuluş GÖLCÜK \_\_\_\_\_

Assist. Prof. Şirin KORULU KOÇ \_\_\_\_\_

It is approved that this thesis has been written in compliance with the formatting rules laid down by the Graduate School of Sciences and Engineering.

\_\_\_\_\_  
Prof. Nurullah ARSLAN  
Director

September 2015

# **AMPEROMETRIC BIOSENSOR FOR DETECTION OF XANTHINE LEVEL FOR MEAT FRESHNESS CONTROL**

Muamer DERVISEVIC

M.S. Thesis – Genetics and Bioengineering  
September 2015

Thesis Supervisor: Assoc. Prof. M. Fatih ABASIYANIK

Co-Supervisor: Assoc. Prof. Mehmet ŞENEL

## **ABSTRACT**

The main goal of this thesis is to fabricate a sensitive and novel amperometric biosensor for detection of xanthine. Xanthine is a byproduct of ATP degradation and important indicator of meat spoilage as such very important molecule to be detected in meat freshness control. Amperometric biosensor was developed by preparation of nanocomposite film which is constructed by separate embedding of reduced expanded graphene oxide (REGO), reduced expanded graphene oxide-Gold (REGO-Au), reduced expanded graphene oxide-Palladium (REGO-Pd), and reduced expanded graphene oxide-Platinum (REGO-Pt) into poly(glycidyl methacrylate-co- vinylferrocene) (P(Vfc<sub>0.4</sub>-GMA)), and by covalent immobilization of Xanthine Oxidase (XOD) on the surface of nanocomposites coated electrode. Using these tailored nanocomposites and surface binding of XOD, it has been systematically studied to obtain optimum and most ideal system for xanthine detection in real samples. Biosensor showed excellent analytical performance in detection of xanthine with sensitivity of 21.98 $\mu$ A/ $\mu$ M, linear range 1 $\mu$ M to 40 $\mu$ M, fast response time of 2s and low detection limit 0.003 $\mu$ M.

**Keywords:** Biosensors, Xanthine, Xanthine Oxidase, graphene, nanocomposites, reduced expanded graphite oxide

# ET TAZELİĞİNİN KONTROLÜ AMAÇLI KSANTİN SEVİYESİNİN ÖLCÜMESİNDE AMPEROMETRİK BİYOSENSÖR GELİŞTİRMESİ

Muamer DERVİSEVIC

Yüksek Lisans Tezi – Genetik ve Biyomühendisliği  
Eylül 2015

Tez Danışmanı: Doç. Dr. M. Fatih ABASIYANIK

Eş Danışman: Doç. Dr. Mehmet ŞENEL

## ÖZ

Sunulan tezin temel amacı, ksantin tayinini yapan yeni ve hassas nitelikli amperometrik biyosensör üretmektir. Ksantin, ATP parçalanma sürecinin bir yan ürünü olup etin bozulduğunu göstermesinden, et tazelik kontrol sürecinde tayini önemli olan bir faktördür. Amperometrik biyosensör, poli(glisidil metakrilat-ko-vinylferosen) (P(Vfc<sub>0,4</sub>-GMA))'in içinde ayrıık gömülü olan indirgenip açılmış grafen oksit (REGO), indirgenip açılmış grafen oksit-Altın (REGO-Au), indirgenip açılmış grafen oksit-Palladyum (REGO-Pd) ve indirgenip açılmış grafen oksit-Platin (REGO-Pt) türevlerinden oluşan nanokompozit filmlerle kaplı olan elektrod yüzeylerine Ksantin Oksidaz'ın (XOD) kovalent immobilizasyonu ile geliştirilmiştir. Oluşturulan nanokompozit ve XOD'in yüzeye bağlanma özellikleri kullanılarak gerçek örneklerde ksantin tayinin optimum şekilde gerçekleşmesi için sistematik çalışmalar yapılmıştır. Biyosensör 21.98uA/uM hassasiyet, 1uM-40uM arasındaki doğrusal ölçüm, 2 saniyelik yanıt süresi ve 0.003uM saptama sınırı ile üstün analitik performans sergilemiştir.

**Anahtar Kelimeler:** Biyosensör, Ksantin, Ksantin Oksidaz, grafen, nanokompozit, indirgenip açılmış grafen oksit

To my parents Senada and Nazif,  
sister Emina, brother Mezen  
and wife Esma

## ACKNOWLEDGEMENT

All the praises and thanks be to Allah SWT, Most Gracious, Most Merciful, Who guided me and guides me, and all the praises and thanks to Him for giving me chance to see, understand, and study science as well for meeting beautiful people with who I work and will be working with. I wish to express my gratitude to my supervisor Assoc.Prof. M. Fatih ABASIYANIK for his help, support and guidance in this thesis work. I would also like to thank to Assoc. Prof. Mehmet ŞENEL who encourage me, who was abundantly helpful and gave me psychological, material and knowledge support whenever I needed it. Thanks go to my friend Emre Çevik (Phd) and my wife Esma Dervisevic (MS) for their knowledge support, encouragement and technical assistance in experimental works, additionally special thanks go to Assist Prof. Zehra Durmuş for providing modified REGOs and their characterizations. Lastly, but not in sense the last, I express my thanks and appreciation to my family for their understanding and support.

## TABLE OF CONTENTS

ABSTRACT.....	iii
ÖZ .....	iv
DEDICATION.....	v
ACKNOWLEDGEMENT .....	vi
TABLE OF CONTENTS.....	vii
LIST OF TABLES .....	x
LIST OF FIGURES .....	xi
LIST OF SYMBOLS AND ABBREVIATIONS .....	xiii
CHAPTER 1 INTRODUCTION.....	1
1.1 Significance of Xanthine.....	3
1.2 Xanthine Detection Methods.....	4
1.2.1 Enzymatic Fluorometric .....	5
1.2.2 Enzymatic Colorimetric .....	5
1.2.3 Capillary Electrophoresis .....	5
1.2.4 High Performance Liquid Chromatography (HPLC).....	6
1.2.5 Mass Spectrometry .....	6
1.2.6 Capillary Column Gas Chromatography .....	6
1.2.7 Mass Fragmentography .....	7
1.2.8 Electrochemical Determination of Xanthine .....	7
CHAPTER 2 AMPEROMETRIC BIOSENSORS.....	8
2.1 Biological Recognition Elements.....	8
2.1.1 Enzymes .....	8
2.1.2 Antibodies .....	9
2.1.3 Nucleic Acids .....	9
2.1.4 Microorganisms.....	9
2.1.5 Tissue Materials .....	10

2.2 Immobilization Techniques.....	10
2.2.1 Covalent Bonding.....	10
2.2.2 Cross-Linking.....	11
2.2.3 Adsorption.....	11
2.2.4 Encapsulation.....	11
2.2.5 Entrapment.....	11
2.3 Polymeric Mediators.....	12
2.4 Graphene and its Nanocomposites.....	13
CHAPTER 3 EXPERIMENTAL.....	15
3.1 Materials.....	15
3.2 Instrumentation.....	15
3.3 Methods.....	16
3.3.1 Synthesis.....	16
3.3.1.1 Synthesis of poly(GMA-co-VFc).....	16
3.3.1.2 Synthesis of REGO Graphene.....	17
3.3.1.3 Synthesis of REGO Graphene Gold.....	17
3.3.1.4 Synthesis of REGO Graphene Platinum.....	17
3.3.1.5 Synthesis of REGO Graphene Palladium.....	18
3.3.2 Preparation of Enzyme Electrode.....	18
3.4 Characterization of Biosensor.....	18
3.5 Determination of Experimental Variables.....	19
3.6 Operational and Storage Stability.....	19
3.6.1 Reusability.....	19
3.6.1 Storage Stability.....	19
3.7 Amperometric Measurements.....	19
3.8 Interference.....	20
3.6 Real-sample Application.....	20
CHAPTER 4 RESULTS AND DISCUSSION.....	21
4.1 Characterizations.....	21
4.1.1 Spectroscopic Results.....	21
4.1.1.1 Fourier transform infrared spectroscopy (FT-IR).....	21
4.1.1.1.1 Reduced Expanded Graphene Oxide (REGO).....	21
4.1.1.1.2 Reduced Expanded Graphene Oxide- Gold (REGO-Au).....	23

4.1.1.1.3 Reduced Expanded Graphene Oxide-Palladium (REGO-Pd).....	24
4.1.1.1.4 Reduced Expanded Graphene Oxide-Platinum (REGO-Pt) .....	25
4.1.1.2 RAMAN Analysis of EG, EGO and REGO .....	26
4.1.1.3 UV Analysis of EG, EGO and REGO .....	27
4.1.1.4 X-ray powder diffraction (XRD) .....	28
4.1.1.4.1 Reduced Expanded Graphene Oxide(REGO).....	28
4.1.1.4.2 Reduced Expanded Graphene Oxide- Gold (REGO-Au) .....	29
4.1.1.4.3 Reduced Expanded Graphene Oxide-Palladium (REGO-Pd).....	30
4.1.1.4.4 Reduced Expanded Graphene Oxide-Platinum (REGO-Pt) .....	31
4.1.2. Electrochemical .....	32
4.1.2.1 Cyclic Voltammogram .....	32
4.1.2.2 Electrochemical Impedance Spectra.....	35
4.1.3 Morphological properties .....	37
4.1.3.1 SEM Analyses .....	37
4.1.3.1.1 EG, EGO and REGO .....	37
4.1.3.1.1 REGO-Au, REGO-Pd and REGO-Pt .....	38
4.1.3.2 TEM Analyses .....	39
4.2 Determination of Experimental Variables .....	40
4.2.1 Optimum pH.....	40
4.2.2 Optimum Temperature .....	42
4.3 Amperometric Response of Bionanocomposite Electrodes.....	43
4.4 Operational and Storage Stability .....	48
4.4.1 Reusability.....	48
4.4.2 Storage Stability .....	49
4.5 Analytical Performance .....	50
4.6 Interference .....	51
4.7 Real-sample Application .....	53
CHAPTER 5 CONCLUSIONS .....	55
REFERENCES .....	57

## LIST OF TABLES

### TABLE

4.1	$R_{ct}$ values of modified electrodes with different bionanocomposite .....	36
4.2	Comparison of analytical performance of proposed xanthine biosensor with biosensors in literature .....	45
4.3	Comparison of analytical performance of proposed xanthine biosensors .....	47
4.4	Analytical performance and efficiency in detection of xanthine of proposed biosensors.....	50

## LIST OF FIGURES

### FIGURE

1.1	Statistical data of meat supply quantity.....	2
1.2	Decomposition of adenosine triphosphate (ATP) in meat spoilage process ....	4
4.1	FT-IR spectrum of EGO and REGO .....	21
4.2	FT-IR spectrum of REGO-Au .....	23
4.3	FT-IR spectrum of REGO-Pd .....	24
4.4	FT-IR spectrum of REGO-Pt .....	25
4.5	RAMAN spectrum of EG, EGO and REGO.....	26
4.6	UV analysis of EG, EGO and REGO.....	27
4.7	XRD patterns of A) EG, B) EGO and C) REGO .....	28
4.8	XRD patterns of REGO-Au .....	29
4.9	XRD patterns of REGO-Pd.....	30
4.10	XRD patterns of REGO-Pt.....	31
4.11	Cyclic voltammograms of biosensors .....	32
4.12	Cyclic voltammograms scan rate of fabricated electrodes.....	33
4.13	Electrochemical Impedance Spectra .....	35
4.14	SEM analyses of EG, EGO and REGO.....	37
4.15	SEM analyses of A) REGO-Au, B) REGO-Pt, C) REGO-Pd .....	38
4.16	TEM analyses of A) REGO-Pt, B) REGO-Pd and C) REGO-Au .....	39
4.17	The effect of buffer pH on the response of biosensors .....	40
4.18	Temperature effect on amperometric response .....	42
4.19	Amperometric response of proposed electrodes .....	43
4.20	Calibration curves for the amperometric response of biosensors .....	46

4.21	Operational stability of enzyme electrode .....	48
4.22	Storage stability of enzyme electrode .....	49
4.23	Interference effect of Glucose, SB, AA, UA.....	51
4.24	Determination of xanthine in beef and chicken meat samples .....	53

## LIST OF SYMBOLS AND ABBREVIATIONS

### SYMBOL/ABBREVIATION

AA	Ascorbic Acid
ADP	Adenosine Di Phosphate
AMP	Adenosine Mono Phosphate
ATP	Adenosine Tri Phosphate
CV	Cyclic Voltammogram
CZE	Capillary Zone Electrophoresis
DL	Detection Limit
DNA	Deoxyribonucleic Acid
DW	Distilled Water
EG	Expanded Graphite
EGO	Expanded Graphite Oxide
EIS	Electrochemical Impedance Spectroscopy
FTIR	Fourier Transform Infrared Spectroscopy
GMA	Glycidyl Methacrylate
HPLC	High Performance Liquid Chromatography
Hx	Hypoxanthine
IMP	Inosine Mono Phosphate
LR	Linear Range
MECC	Micellar Electrophoretic Capillary Chromatography
PBS	Phosphate Buffered-Saline
PGE	Pencil Graphite Electrode
PGE	Pencil Graphite Electrode
REGO	Reduced Expanded Graphene Oxide

REGO-Au	Reduced Expanded Graphene Oxide-Gold
REGO-Pd	Reduced Expanded Graphene Oxide-Palladium
REGO-Pt	Reduced Expanded Graphene Oxide-Platinum
RNA	Ribonucleic Acid
RT	Response Time
SB	Sodium Benzoat
SEM	Scanning Electron Microscopy
TEM	Transmission Electron Microscopy
UA	Uric Acid
UV	Ultra Violet
Vfc	Vinyl ferrocene
Xn	Xanthine
XO	Xanthine Oxidase
XRD	X-ray Powder Diffraction

## **CHAPTER 1**

### **INTRODUCTION**

Meat and meat products are currently one of the most important components of a healthy and well balanced diet due to its nutritional richness (Pereira and Vicente, 2013) and since the meat quality reduction directly affects consumers, being the last step of the production chain, the necessary safety rules should be taken into consideration. The need for keeping freshness of meat on acceptable quality level is of highly importance in food industries to manufacture safe and qualified products, especially when meat consumption rapidly increases as population increases. In order to visualize meat consumption cutler in the world in figure 1.1 statistical data is presented. Worlds meat-food supply quantity in years of 1990 ( $175 \times 10^6$  tones), 2000 ( $225 \times 10^6$  tones) and 2011 in which was more than 290 million tones consumed (FAOSTAT, 2014), which demonstrates that meat consumption increased almost 40% in last 20 years. Statistical data (see Figure 1.1 B) of the consumption of meat supply quantity per individual in a day (gram/capita/day at average) for different regions of the world; Europe, America, Oceania, Asia and Africa in the years of 1990, 2000 and 2011, shows that meat consumption slowly increases. In certain regions such as Asia and Africa meat consumption in last 20 years are 66 and 45 gram/capita/day (average in 20 years) which are significantly smaller than in Europe, America and Oceania, with values of 205, 217 and 294 gram/capita/day (average in 20 years). Regardless to economical status, production power, population size and meat consumption culture they all have increment in meat consumption or large quantity of meat consumption daily.

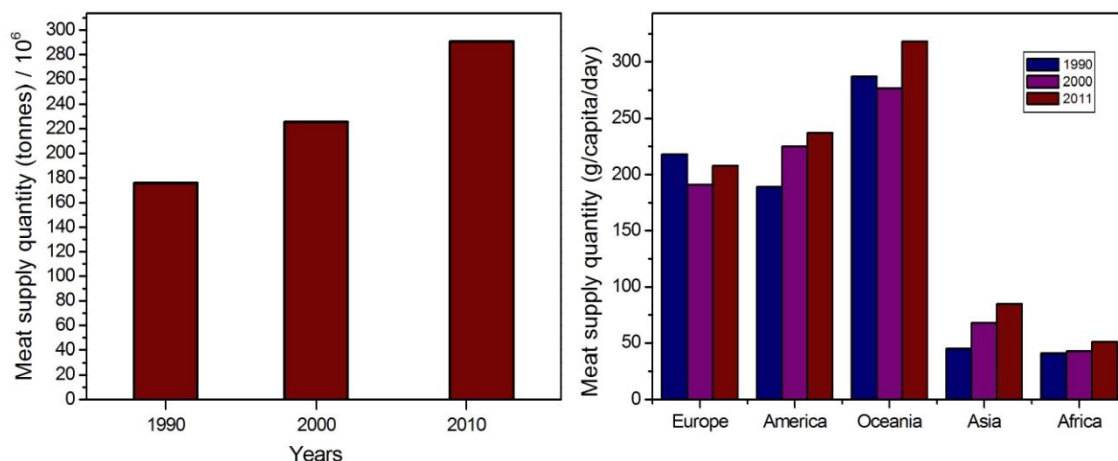


Figure 1.1 A) Statistical data of meat supply quantity (tones 10<sup>6</sup>) in world, presenting consumption in the years of 1990, 2000, 2011 B) Statistical data of meat supply quantity (gram/capita/day) consumption in years of 1990, 2000 and 2011 in Europe, America, Oceania, Asia, Africa, (data values obtained from FAOSTAT, Food and Agriculture Organization of the United Nations)

Next to enormous numbers in meat consumption, importance of meat nutritional composition and nutritive role in the human diet is reviewed by Pereira and Vicente (2013). Meat spoilage is not always evident and with gross discoloration, strong off-odors, and the development of slime would constitute the main qualitative criteria for meat rejection which may be found in meat during inappropriate distribution, which is reviewed in details by Nychas et al., (2008). Food industry, evaluates the quality of a product through periodic chemical and microbiological analysis, using conventionally techniques such as, chromatography, spectrophotometry, electrophoresis, titration and others, which do not allow an easy continuous monitoring; because of their high expense, time consuming, a need for well trained personnel and in some cases requires steps of extraction or sample pretreatment which additionally increases analysis time (Mello and Kubota, 2002). In the time of unceasing technological development, construction of small compact amperometric biosensor for cheap and continuous monitoring, with fast response time, low detection limit, high sensitivity and easy to operate with, can easily overcome above limitations. Combination of complex chemical, microbiological and physical processes leads to loss of freshness and finally to spoilage, and most important criterion in quality is to ensure that quality of meat meets high criterion on daily routine basis (Sadeghi et al., 2014)

## 1.1 SIGNIFICANCE OF XANTHINE

Hypoxanthine is a minor constituent of its nucleoside, inosine in transfer RNA (Lawal and Adeloju, 2012a), and it has been found to accumulate in meat and in organs such as kidney, skeletal muscle and heart (Lawal and Adeloju, 2012b, Yano et al., 1995), and it is catalyzed by xanthine oxidase into xanthine and uric acid (see Figure 1.1.2). Xanthine is an intermediate of the purine nucleotide and deoxynucleotide metabolism (Luong et al., 1989) and as the metabolic precursor of uric acid, it is the first indicator of an abnormal purine profile and can serve as a marker of various diseases (Kalimuthu et al., 2012) such as xanthinuria (Kawachi et al., 1990), gout (Kim et al., 2003), cerebral ischemia (Ono et al., 2009), hyperuricemia (Campion et al., 1987), perinatal asphyxia (Banupriya et al., 2008), pre-eclampsia (McMaster, 2008), tumorhyperthermia (Frank et al., 1998) etc.. In the food industry elevated levels of hypoxanthine and xanthine as important biomarkers are a sign of spoilage (Carsol et al., 1997). Schematic representation (see Figure 1.2) shows ATP decomposition during meat spoilage and generation of hypoxanthine and xanthine through xanthine oxidase (XO), respectively. After xanthine is converted to uric acid by XO and is excreted through urine. The important point in this process is the oxidation of hypoxanthine by xanthine oxidase in order to form xanthine and uric acid, from which it is easy to consequently monitor concentration of hypoxanthine and predict time of death of fish or animal (Lawal and Adeloju, 2012a), as well hypoxanthine has huge effect on meat flavor. Although the flavor of meat develops largely through cooking process, IMP is a major contributing factor to flavor of meat freshness and its degraded product hypoxanthine imparts the bitter taste of meat (Mulchandani et al., 1989), as well as fresh meat contains nonvolatile constituents that are essential flavor precursors and contribute to the basic taste of cooked meat (MacLeod, 1986; Tikik et al., 2006).

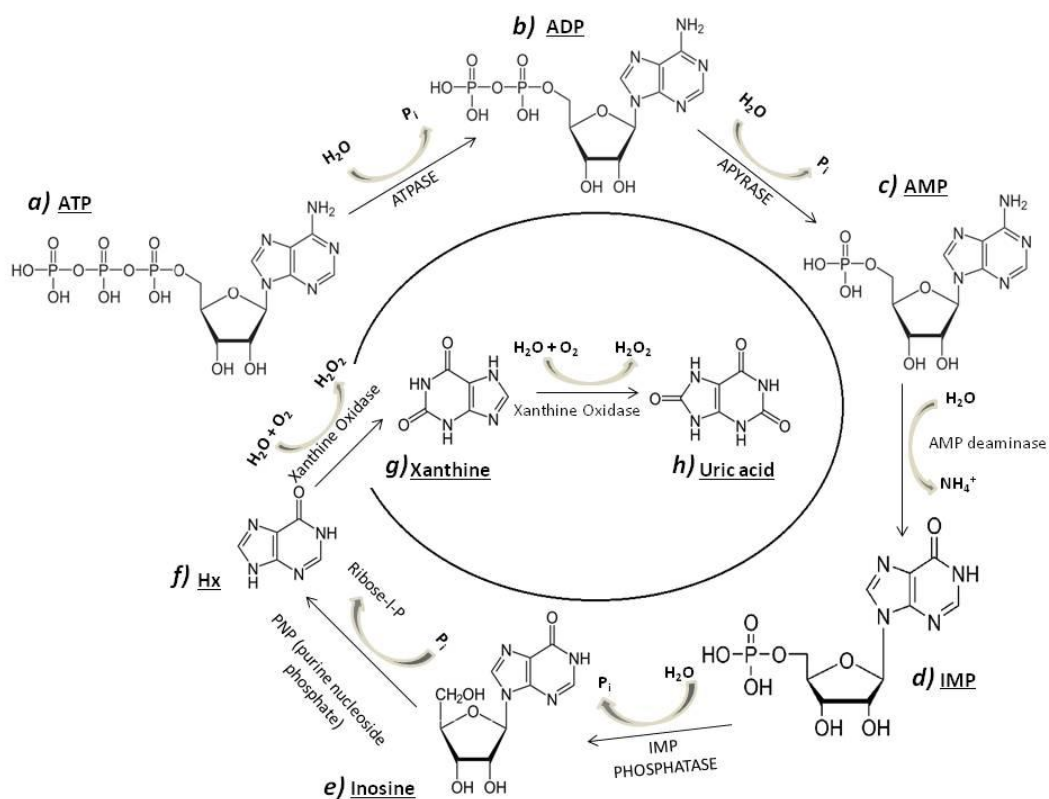


Figure 1.2 Decomposition of adenosine triphosphate (ATP) during meat spoilage process, a) ATP, b) adenosine diphosphate (DTP), c) adenosine monophosphate (AMP), d) Inosine monophosphate (IMP), e) Inosine, f) Hypoxanthine (Hx), g) Xanthine, h) Uric acid (UA).

## 1.2 XANTHINE DETECTION METHODS

According to the literature, there have been various methods used for xanthine determination named as enzymatic fluorimetric (Beckman et al., 1989), enzymatic colorimetric (Berti et al., 1988, Litwack et al., 1953), capillary electrophoresis (Chen et al., 2002, Caussé et al., 2007), high performance liquid chromatography (HPLC) (Cooper et al., 2006, Kock et al., 1993), mass spectrometry (Parker et al., 1969, Rashed et al., 2005), capillary column gas chromatography (Renata et al., 2002), and mass fragmentography (Olojoa et al., 2005). To the contrary of considerable amount in the number of diverse xanthine detection methods published, commercially available methods which include fluorometric and spectrometric are not easily commercialized comparing to electrochemical methods

The methods stated above require tedious sample preparation steps, expensive equipment, trained people and long operation time (Devi et al., 2012a).

### **1.2.1 Enzymatic Fluorometric**

Enzymatic fluorometric assays are based on difference in fluorescence of substrate from product used to measure reaction which is more sensitive than spectrophotometric assays, however their disadvantage is that results can hugely suffer from interference. In xanthine detection, xanthine oxidase catalyzes conversion of pterin to isoxanthopterin which give basis for fluorometric assay (Beckman et al., 1989). Although this method is 100 to 500 times more sensitive than spectrophotometric, unfortunately its long reaction periods leads to conversion of xanthine dehydrogenase to oxidase (Beckman et al., 1989). It has been successfully applied to the areas where xanthine dehydrogenase and oxidase activities are too low such as brain and kidney.

### **1.2.2 Enzymatic Colorimetric**

Enzymatic colorimetric assay is enzymatic analysis widely used in diagnostic laboratories and it is based on reaction color proceeded by an enzyme-catalyzed reaction. A colorimetric method for xanthine involves the precipitation of the purine bases as their sopper salts (Horecker et al., 1949), as well involves precipitation of the proteins in aliquots of the incubating homogenate system (Litwack et al., 1953). Measuring xanthine oxidase activity in homogenate systems is desirable after disappearance of substrate for several reasons: i) the development of a color reaction, ii) large endogenous respiration, and iii) the presence of uricase complicates the measurements of uric acid formation (Litwack et al.,1953).

### **1.2.3 Capillary Electrophoresis**

Capillary electrophoresis is a separation method preformed in submillimeter diameter capillaries from which very often capillary zone electrophoresis (CZE) and micellar electrokinetic capillary chromatography (MECC) are used. Capillary electrophoresis method has been employed for separation of xanthine, haypoxanthine, guanine, adenine, uric acid and theophylline (Chen et al., 2002).

Factors which are of high importance and should be paid attention to are separation voltage, injection time and detection potential, acidity, and concentration of running buffer which has to be optimized. This method gives ability to separate the six purine bases within 14 min (Chen et al., 2002) which is very long.

#### **1.2.4 High Performance Liquid Chromatography (HPLC)**

High performance liquid chromatography is an analytical technique used to identify, separate, and quantify each component in mixture based on adsorbent material with which column are filled in and pumps which are pressurizing liquid solvent containing mixture through columns. Uric acid, xanthine, and hypoxanthine validation in human serum have some issues which has to be addressed, such as potential matrix lots of interference, sample concentration range, substitution of analyte free matrix standard preparation and variation endogenous concentrations (Cooper et al., 2006). However, this kind of method requires professional personnel, high-tech equipment and it is not convenient for onsite detection.

#### **1.2.5 Mass Spectrometry**

Mass spectrometry is a technique used in analytical chemistry for identification of type and amount of chemicals present in sample which is based on abundance of gas phase ions as well by measuring the mass to charge ratio with a mass spectrum function represented in ion signals. Identification of xanthine and hypoxanthine in urine through analysis including mass spectrometry are carried out in negative ion selected reaction monitoring mode (Rashed et al., 2005). Because turnaround time is 7 min, stable isotope dilution used in such a method is simple, specific and rapid, it provides reliable results in diagnosis for molybdenum cofactor and isolated sulphite oxidase deficiencies (Rashed et al., 2005). Disadvantages of this method are huge equipment, long sample preparation and needed well skilled personnel.

#### **1.2.6 Capillary Column Gas Chromatography**

Capillary column gas chromatography is a method used for analyzing and separating compounds that can be vaporized without decomposition usually including testing of purity of particular substance. One of the examples of usage of capillary column gas chromatography is reported by Peck et al., in determination of nitrated

polynuclear aromatic hydrocarbons (Peck et al., 1983). As far for xanthine application Renata et al., reported a study on a quantitative method for the analysis of xanthine alkaloids in *Paullinia cupana* (guarana) by capillary column gas chromatography (Renata et al., 2002).

### **1.2.7 Mass Fragmentography**

Mass fragmentography is a method made of combination of gas chromatography and mass spectrometry and usually is used to quantify and isolate ionic fragments' characteristics of certain compound by investigation of ions having mass to charge ratio. This method does not need previous separation of substances since it has selection of accurate mass peaks, however it does involve tedious equipment calibration (Chabard et al., 1980). This method allows obtaining accurate and relatively homogeneous results and as well proofing to be extremely effective in development of oxypurines serum concentrations (Chabard et al., 1980).

### **1.2.8 Electrochemical Determination of Xanthine**

Electrochemical methods are electrochemistry analysis concerned with the interrelation of chemical and electrical effects. One of the most applied electrochemical methods in biosensors is amperometric analysis. There is big interest going on related to amperometric biosensor for xanthine detection. In the time of technological development explosion, amperometric biosensors are one of the best candidates for constructing compact, cheap, continuous motoring, fast response, low detection limit, high sensitivity and selectivity, easily to operate and in general easily overcomes all limitations in methods described above (Dervisevic et al., 2015a). Application of amperometric method in xanthine determination is largely in literature (see Table 4.3.1) which are based on conducting polymers or in some cases nanocomposite and xanthine oxidase.

## **CHAPTER 2**

### **AMPEROMETRIC BIOSENSORS**

Biosensors are a compacted analytical device which is composed of biological derived sensitive recognition element (Yoo and Lee, 2010) connected to or integrated within a physio-chemical transducer (Gerard et al., 2002). They have three main parts: biological recognition element which recognizes the target molecule in the presence of various chemicals, a transducer that converts the bio-recognition event into a measurable signal, and a signal processing system that converts the signal into readable form (Clark and Lyons, 1962, Updike and Hicks, 1967, Hiratsuka, et al., 2008, Yoo and Lee, 2010). Because of their performance, including; high sensitivity, greater analytic discrimination (Li et al., 2010), rapid response, low operating costs, compact size and user-friendly operation, they have become an important tool for detection of chemical and biological components for food, environmental and clinical monitoring (Aziz et al., 2006).

#### **2.1 BIOLOGICAL RECOGNITION ELEMENTS**

##### **2.1.1 Enzymes**

Enzymes are large complex macromolecules which are largely composed of proteins and often include prosthetic group which includes one or more metallic atoms. Enzymes used in biosensors involve oxidation or reduction mode which can be consistently followed electrochemically, for example Xanthine Oxidase, Glucose Oxidase, Cholesterol Oxidase etc. Advantages of enzymes in biosensors are that they

can bind to substrate easily, highly selective, fast acting, they have catalytic activity and most commonly used in amperometric biosensors. However, they are expensive and they tend to loss activity when they are immobilized on a polymer, or can be deactivated after a relatively short period of time, if not optimized carefully.

### **2.1.2 Antibodies**

Antibodies are the most versatile biological recognition agent which can be developed against almost any substance thus making them highly sensitive, specific and selective material. Antibodies are usually used in biosensors for detection of cancer markers which can be proteins or even cancer cells and they can be immobilized and used with almost all transducers. Their ability to perfectly select between different strains and bind very powerfully makes them ultra sensitive and reliable whereas antibody will detect any compound binding to receptor (Taylor et al., 1991). However their production is of high cost and their special disadvantage is that they don't have catalytic effect.

### **2.1.3 Nucleic Acids**

Nucleic acids in biosensors are usually compared with antibodies because they can operate in many ways, as well specific base-pairing. Usually they are used to detect genetic diseases, viral infections and cancer markers and because of their various labeling ability such as photometric, radioactive, electro-active or enzymic and by that giving them a scope for wide biosensor applications. Utilization of DNA or RNA strands as probes for sensing and target recognition happens in two ways; first hybridization of probes which is based on a wide range of sensor and second association with targets by relating to the specific properties of target (Chao et al., 2015). Unlike common biosensors, nucleic acids based biosensors are with high sensitivity, low cost and high assembly efficiency.

### **2.1.4 Microorganisms**

Microorganisms are playing an important role in biotechnology processes and industry. Huge number of biosensors has been designed by simple immobilization of microorganism on electrode surface to assist monitoring various processes in many fields such as food manufacturing, pharmaceutical synthesis, energy production and waste-water treatment. Advantages of microbial biosensor are that they have long

lifetime, cheaper source of enzymes, more tolerant to environment (Eggins, 2011). It should be noted that they do have long response, have long recovery time and they have less selectivity because various enzymes inside organism.

### **2.1.5 Tissue Materials**

Animal and plant tissues can be used in biosensor applications because generally tissues contain multiple enzymes which exist in natural environment as such less subjected to degradation. Both microorganisms and tissues are enzyme containing materials the difference is that a different environment surrounding the enzyme comes up with different results. In tissue materials the major disadvantage is losing of selectivity as for an example, banana tissue based biosensors for dopamine determination had many interfering molecules. As advantages they are good for enzyme maintenance in their natural environment, enzymes are much cheaper than purified ones, enzyme activity is stable (Eggins, 2011).

## **2.2 IMMOBILIZATION TECHNIQUES**

Immobilization techniques are core of biosensor fabrication, because just selecting efficient biological recognition element is not enough, but attaching it to the electrode surface is as much of high importance. Immobilization methods used in biosensor fabrication are covalent bonding, entrapment, adsorption, cross-linking, and encapsulation.

### **2.2.1 Covalent Bonding**

Covalent bonding is the method which is mostly desired in enzyme based biosensors fabrication. In this method bonds occur between functional groups which are not essential for catalytic activity of enzyme providing covalent bound of enzyme to the electrode surface (Sassolas et al., 2012). Process of binding enzyme to the solid support is carried out by initial surface activation, followed by enzyme coupling, then removal of unbound biomolecules (Sassolas et al., 2012). Covalent immobilization can be performed directly to the transducer irrespectively to the carrier support which can be natural, inorganic material, or synthetic polymer (Sassolas et al., 2012). This method

requires optimal conditions for performing reaction, such as pH, temperature, low ionic strength etc (Zhao and Jiang, 2010).

### **2.2.2 Cross-Linking**

The cross linking is the method in which biomaterial is chemically bounded to solid for supporting material such as cross-linking agent glutaraldehyde, as well it should be avoided because this agent can interfere with enzymatic activity (Zhao and Jiang, 2010). This method has proven to be useful in methods for enzyme immobilization because of its simplicity and strong chemical bonds (Sassolas et al., 2012). The main disadvantage of this method is that enzyme activity is lost due to distortion of enzyme conformation (Sassolas et al., 2012).

### **2.2.3 Adsorption**

Adsorption is the simplest and fastest way to immobilize biological recognition element to the electrode surface (Sassolas et al., 2012), and it is the simple adhesion of atoms, ions or biomolecules (Brandt et al., 1993). Adsorption can be simply divided into i) physical adsorption which is weak and mainly occurs via Van der Waals mostly used for enzyme immobilization and ii) chemical adsorption which is stronger and involves the formation of covalent bonds (Zhao and Jiang, 2010).

### **2.2.4 Encapsulation**

Encapsulation includes the trapping biological recognition elements within capsules of different composition. Since it is very similar to entrapment it has common properties with extra protection of purified enzymes from unfolding, degradation, and ensures large activity time. Although, it can provide selectivity, response time is very long and it's hard to apply on onsite.

### **2.2.5 Entrapment**

Entrapment refers to mixture of biomaterials and then polymerized to a gel (Zhao and Jiang, 2010), by immobilizing biological recognition element in three-dimensional matrices (Sassolas et al., 2012). Immobilization by entrapment method is easy to perform as well simultaneous deposition in the same sensing layer such as mediators and other additives is possible. Advantages of this method are that there is no modification of the biological recognition elements and enzyme is preserved during

immobilization process as well shell life is longer (Sassolas et al., 2012). However, entrapments method can give rise to barriers to the diffusion of substrate (Zhao and Jiang, 2010), by that the performance of the system will be restricted (Sassolas et al., 2012).

### **2.3 POLYMERIC MEDIATORS**

The efficiency of amperometric xanthine biosensors is much better than techniques described above, but there is a challenge inside the field of amperometric biosensors, and it is not just enzyme immobilization on electrode surface but also to enhancement of communication between electrode and enzyme by making electron transfer faster. Xanthine oxidase is important part of the xanthine biosensor but its full efficiency is occurring when applied with conducting polymers. Flexibilities provided by conducting polymers in chemical structures modification have offered a great deal for novel applications in various fields. Mediators are electron transfer agents that are able to participate in the redox reaction together with biological molecules and thus improving electron transfer (Chaubey and Malhotra, 2002). Basically they are a low molecular weight redox couple which shuttles electrons with high speed from the redox of the enzyme towards the electrode surface. These redox couples are supposed to be stable under required working conditions and should not participate in side reactions (Chaubey and Malhotra, 2002). Characteristics of ideal mediator are; i) having stable oxidation and reduction forms, ii) its reduced form should not react with oxygen, iii) being pH independent and low potential for oxidizing mediators, and iv) reacting rapidly with reduced enzyme (Chaubey and Malhotra, 2002). Advantages of using mediators are that the measurements are less depended on oxygen concentration, low oxidation potential is applied to avoid interference, working potential is determined by the oxidation potential of mediator and oxidation of reduced mediators does not involve protons (Chaubey and Malhotra, 2002).

## 2.4 GRAPHENE AND ITS NANOCOMPOSITES

Graphene is a real two-dimensional structure (one-atom-thick) and comprises a single  $sp^2$ - hybridized carbon atoms joined by covalent bonds (Zhigang et al., 2012), with high crystal quality and exhibits quite unusual electronic properties (Hongmin et al., 2013). Graphene is an excellent conductor, heterogeneous electron transfer occurs at edge of graphene (Ostrovsky et al., 2006), it contains a large number of defects and large number electroactive sites in big area graphenes (Pumera, 2010), and electrodes made from it, have much more electrochemically active sites than graphite ones (Du et al., 2004, Abdulazeez, 2015). However, the electrochemical properties of graphene are not clearly understood, although a lot of studies showed that fast electron transfer between enzymes and electrodes can be obtained due to the unique electronic structure of graphene (Zhigang et al., 2012, Tang et al., 2009, Shang et al., 2008 McCreery, 2008). This is mainly caused by delocalized  $\pi$  bonds above and below the basal plane and delocalized electrons create high electrical conductivity and mobility for graphene within the plane (Zhigang et al., 2012, Yang et al., 2010), thus usage of graphene in biosensors application can solve problems related to transition metals, like Ni, Fe, Co, etc. Graphenes excellent thermal conductivity, mechanical flexibility, excellent chemical tolerance, high surface to volume ratio, and most important fast electron transportation and good biocompatibility make the graphene an attractive matrix for composites an ideal candidate for biosensing application. Thus, it is desirable to use a low-cost, facile and effective approach, such as soluble reduced graphene oxide (REGO) sheets in high quantity, for biosensor applications, which can be produced by thermal annealing reduction (Farnaz et al., 2015). As it can be seen in literature graphene has important role in biosensor applications, for example, Chiu et al., made study on protein immobilization on graphene oxide sheet for the purpose of surface plasmon resonance sensors (Nan-Fu and Teng-Yi, 2014), Zengjie et al., reports a new enzymatic immobilization carrier based on graphene capsule for hydrogen peroxide biosensors (Zengjie et al., 2015), Lorestani et al., publishes work on one-step hydrothermal green synthesis of silver nanoparticle-carbonnanotube reduced-graphene oxide composite and its application as hydrogen peroxide sensor (Farnaz et al., 2015), and Choi et al., reports flow-injection amperometric glucose biosensors based on graphene/Nafion hybrid electrodes (Bong et al., 2011), which all reported application of graphene in different types of biosensors.

Aim of this thesis is to develop amperometric biosensor which is based on REGO-Pt, REGO-Pd and REGO- Au nanocomposites for xanthine detection. Nanocomposites served as an electron transfer enhancer and a material to decrease polymers resistivity, which has been demonstrated through this study.

## CHAPTER 3

### EXPERIMENTAL

#### 3.1 MATERIALS

Xanthine oxidase, xanthine, vinylferrocene (VFc) and Glycidyl methacrylate, Iron (III) nitrate nonahydrate,  $\text{Fe}(\text{NO}_3)_3 \cdot 9\text{H}_2\text{O}$ , iron (II) chlorur tetrahydrate ( $\text{FeCl}_2 \cdot 4\text{H}_2\text{O}$ ), sulfuric acid ( $\text{H}_2\text{SO}_4$  fuming), hydrazine hydrate ( $\text{N}_2\text{H}_4 \cdot \text{H}_2\text{O}$ ), potassium permanganate ( $\text{KMnO}_4$ ), hydrochloric acid (37% HCl), hydrogen peroxide (30%  $\text{H}_2\text{O}_2$ ), sodium nitrate ( $\text{NaNO}_3$ ) and ammonia solution (28%  $\text{NH}_3$ ) were purchased from Merck and Sigma-Aldrich. All the chemicals employed in the study were analytical grade and used as-received without a purification. The EG was a commercial grade, thermally expanded product (TIMREX<sup>®</sup> BNB90), kindly provided by TIMCAL (Switzerland). The density, surface area, average particle size ( $d_{90}$ ) and the oil adsorption number (OAN) values of EG were reported as 2.24 g/cm<sup>3</sup>, 28 m<sup>2</sup>/g, 85.2 μm and 150 ml/100 mg, respectively by the producer.

#### 3.2 INSTRUMENTATION

Electrochemical measurements were performed using CompactSoft portable electrochemical interface and impedance analyser (*Ivium Technologies*) with electrochemical system composed from working, Ag/AgCl reference, and Platinum auxiliary electrodes in the electrochemical cell containing phosphate buffered-saline (PBS) solution. After the working electrode reached the steady state, the redox reaction was initiated with the addition of Xanthine to the unceasingly stirred PBS solution. The amperometric measurements were taken at applied potential of 0.35 V generally at room

temperature except optimum temperature experiments. The substrate solution was prepared by dissolving Xanthine in 30/70% 0.1M NaOH and PBS respectively and was prepared freshly before every measurement. Electrochemical impedance spectroscopy (EIS) measurements were carried out using a CHI Model 6005 electrochemical analyzer in a background solution of 5 mM  $\text{Fe}^{3+}/\text{Fe}^{2+}$  PBS pH 7.0 at 0.35V potential and with alternating voltage of 5 mV and the frequency range of  $5.0 \times 10^{-2}$  to  $1.0 \times 10^6$  Hz. FTIR spectra were recorded in transmission mode with a Bruker Alpha infrared spectrometer using the ATR mode, in the range  $400\text{-}4000\text{ cm}^{-1}$  with the resolution of  $2\text{ cm}^{-1}$ . The XRD patterns of samples were obtained by using a Rigaku Smart Lab. XRD with  $\text{Cu-K}\alpha$  radiation at room temperature. The Raman spectra of graphitic materials were also recorded in a Thermo-Fisher Scientific, DXR dispersive Raman instrument using laser excitation of 532 and 780 nm and an InGaAs detector, in the range of  $400\text{-}3500\text{ cm}^{-1}$ . One hundred scans were accumulated with the resolution of  $4\text{ cm}^{-1}$  with using a 100mW laser power. Spectrophotometric measurements in absorption experiments were carried out using a PerkinElmer Lambda 35 series UV-Visible spectrophotometer with a scan range of  $250\text{-}400\text{ nm}^{-1}$  and a spectral resolution of 1 nm. Two scanning electron microscope (SEM) was employed to observe the surface of the samples. For SEM, pieces of the membranes were mounted on stubs and coated with gold using a sputter coater. SEM micrographs of the samples were taken using a field emission SEM (FESEM, FEI Quanta FEG 450) and a JEOL NeoScope scanning electron microscope operated at 30 kV.

### 3.3 METHODS

#### 3.3.1 Synthesis

##### 3.3.1.1 Synthesis of poly(GMA-co-VFc)

The redox polymer, having different compositions, was prepared according to our earlier study (Dervisevic et al., 2015a). A mixture of VFc and GMA at a known molar ratio was injected into a Pyrex tube, AIBN (1 mol% based on the total monomer concentration was identical for all samples,  $5\text{ mol/dm}^3$ ). The mixture was degassed with Argon and vacuum sealed. Next, the tubes were placed in constant temperature baths, controlled to  $70\text{ }^\circ\text{C}$ . After 2 days, the reaction mixture was added drop wise, while

rapidly stirring the diethyl ether to precipitate the copolymer. The precipitated copolymer was washed with diethyl ether and reprecipitated in this manner, twice, and finally vacuum dried.

### ***3.3.1.2 Synthesis of REGO Graphene***

Synthesis of reduced expanded graphite oxide- grapheme (REGO) was prepared like in our previously reported study (Dervisevic et al., 2015b) which starts with EG oxidation by the well-known modified Hummers (Hummers and Offeman, 1958) method for EGO preparation. In the second step, EGO powder was dispersed in the distilled water in a flask and a stable yellow-brown dispersion was obtained due to the hydrophilic nature of EGO. Most frequently used reducing agent hydrazine monohydrate was added to the EGO suspension, due to the simplicity of its application procedure and the reduction efficiency to obtain graphene sheet having excellent physical properties (Park, et al., 2011). After, the flask equipped with a water-cooled condenser was heated up to 100 °C in an oil bath and kept at this temperature for 24 h. The EGO sheets were reduced to form graphene nano-sheets or reduced expanded graphite oxide, REGO, and gradually precipitated out as a black solid due to the hydrophobic nature of REGO sheets. In the end, the REGO was isolated by filtration and washed with the excess of water and methanol then dried in a vacuum oven.

### ***3.3.1.3 Synthesis of REGO Graphene Gold***

HAuCl<sub>4</sub> aqueous solution was heated to boiling with vigorous stirring, and then a trisodium citrate solution was added. The mixture was kept boiling for 30 min and then allowed to cool to room temperature with continuous stirring. Au nanoparticles were separated by centrifugation and washed several times by distilled water and alcohol.

### ***3.3.1.4 Synthesis of REGO Graphene Platinum***

Graphene (REGO) nano sheets were dispersed in ethylene glycol solution and sonicated for 1 h. Subsequently, proper amount of platinum chloride solution (5 mg/mL) was added to the graphene solution and sonicated for 2 h. The pH of the solution was adjusted to 11 using sodium hydroxide solution and then the solution was stirred under argon atmosphere at 140°C for 5 h. Then freshly made sodium borohydride solution was added with drop-wise to the above solution under vigorous

stirring for 1 h at room temperature. REGO-Pt solid material produced was then centrifuged, washed with deionized water and finally dried in a vacuum oven at 45°C for 24 h.

### ***3.3.1.5 Synthesis of REGO Graphene Palladium***

For the synthesis of the REGO-Pd sample, synthesis protocol of REGO-Pt was modified according to palladium chloride solution.

### **3.3.2 Preparation of Enzyme electrode**

The Pencil Graphite Electrodes (PGEs) were primarily washed with acetone and then with distilled water (DW) to come up with a clean polymer immobilization surface obtained just after remained DW drops evaporate. Afterwards enough volume of well mixed poly(VFc<sub>0.4</sub>-GMA), poly(VFc<sub>0.4</sub>-GMA)/REGO, poly(VFc<sub>0.4</sub>-GMA)/REGO-Au, poly(VFc<sub>0.4</sub>-GMA)/REGO-Pt and poly(VFc<sub>0.4</sub>-GMA)/REGO-Pd were individually cautiously dropped to cover the immobilization surface area of the electrodes. PGEs were left to dry in drying-oven set at 60°C, washed with few drops of 10 mM phosphate buffer saline (PBS) at a pH of 7.0 and then immersed in 9 mg/ml Xanthine oxidase dissolved in PBS solution for 48 h on the orbital shaker set at 200 rpm and placed at 4°C. The working electrodes were rinsed carefully with few drops of PBS prior to be used, and stored in PBS at 4°C while not used.

## **3.4 CHARACTERIZATION OF BIOSENSOR**

Fabricated enzyme electrodes were characterized by electrochemical spectroscopic and morphological analysis. From electrochemical measurements cyclic voltammogram (CV) and electrochemical impedance spectroscopy (EIS) was conducted. In spectroscopic measurements Fourier transforms infrared spectroscopy (FT-IR), RAMAN, UV and X-ray powder diffraction (XRD). Finally for morphological measurements scanning electron microscopy (SEM) and transmission electron microscopy (TEM) were performed.

### **3.5 DETERMINATION OF EXPERIMENTAL VARIABLES**

Experimental variables pH and temperature are conducted under following conditions; i) optimum pH experiments were performed in the range of 5.0 to 9.0 pH PBS 10mM with the applied potential of 0.35V and amperometric current change was recorded ii) optimum temperature experiments were conducted over the temperature range of 25°C to 50°C in pH 7.0 PBS 10 mM with applied potential of 0.35V.

### **3.6 OPERATIONAL AND STORAGE STABILITY**

#### **3.6.1 Reusability**

Operational stability of proposed biosensor was investigated by applying enzyme electrode under consequent amperometric measurements for 20 continue assays. After each assay amperometric current change was recorded and electrode was cleaned with PBS pH 7.0, 10mM and stored in fridge 4°C for 5 minutes. Current change was recorded, respectively.

#### **3.6.2 Storage Stability**

Storage stability was performed over the period of 16 days. Electrodes were stored in fridge 4°C in PBS pH 7.0 10mM and on random days amperometric response was measured and recorded, respectively.

### **3.7 AMPEROMETRIC MEASUREMENTS**

Amperometric measurements were performed using CompactSoft portable electrochemical interface and impedance analyzer (Ivium Technologies). The electrochemical measurements were recorded via a three electrode system set at a working potential of +0.35 V that was composed of Ag/AgCl as reference, Platinum wire as auxiliary, and poly(VFc<sub>0.4</sub>-GMA), poly(VFc<sub>0.4</sub>-GMA)/REGO, poly(VFc<sub>0.4</sub>-GMA)/REGO-Au, poly(VFc<sub>0.4</sub>-GMA)/REGO-Pt and poly(VFc<sub>0.4</sub>-GMA)/REGO-Pd, as working electrodes all immersed in an electrochemical cell filled with 10 mM PBS (pH 7.0). Conventional three-electrode electrochemical cell was purchased from CH Instruments. After allowing the steady-state current to be reached, the Xanthine catalysis were triggered by Xanthine additions to the buffer solution from working cell

being continuously stirred at room temperature. The substrate solution was freshly prepared by dissolving Xanthine in 30/70% 0.1 M NaOH and PBS, and the amperometric responses were recorded with the addition of known amounts of xanthine solution, respectively.

### **3.8 INTERFERENCE**

Interference study was conducted by adding glucose, uric acid (UA), ascorbic acid (AA), sodium benzoate (SB) to the enzyme electrode during amperometric measurements. Substances which can have an interference effect on the current response of the biosensor to xanthine were tested. 1:1 ratio four different interfering substances which are glucose, uric acid (UA), ascorbic acid (AA), sodium benzoate (SB), were used to determine the effect of interference to the biosensor performance respectively.

### **3.9 REAL-SAMPLE APPLICATION**

Chicken and beef meats were purchased from local market, cut into pieces, homogenized, and mixed with DW with a ratio of 1:3 (w/w). Afterwards, the homogenate was filtered with filter paper and content of xanthine was determined by described biosensors under optimal conditions. Xanthine measurements were performed with the samples awaited for 2, 5, 10, 15 and 20 days in fridge at +4°C, and data was interpolated using standard curve (concentration vs current) prepared under optimal working conditions.

## CHAPTER 4

### RESULTS AND DISCUSSION

#### 4.1 CHARACTERIZATIONS

##### 4.1.1 Spectroscopic Results

###### 4.1.1.1 Fourier transform infrared spectroscopy (FT-IR)

###### 4.1.1.1.1 Reduced Expanded Graphene Oxide (REGO)

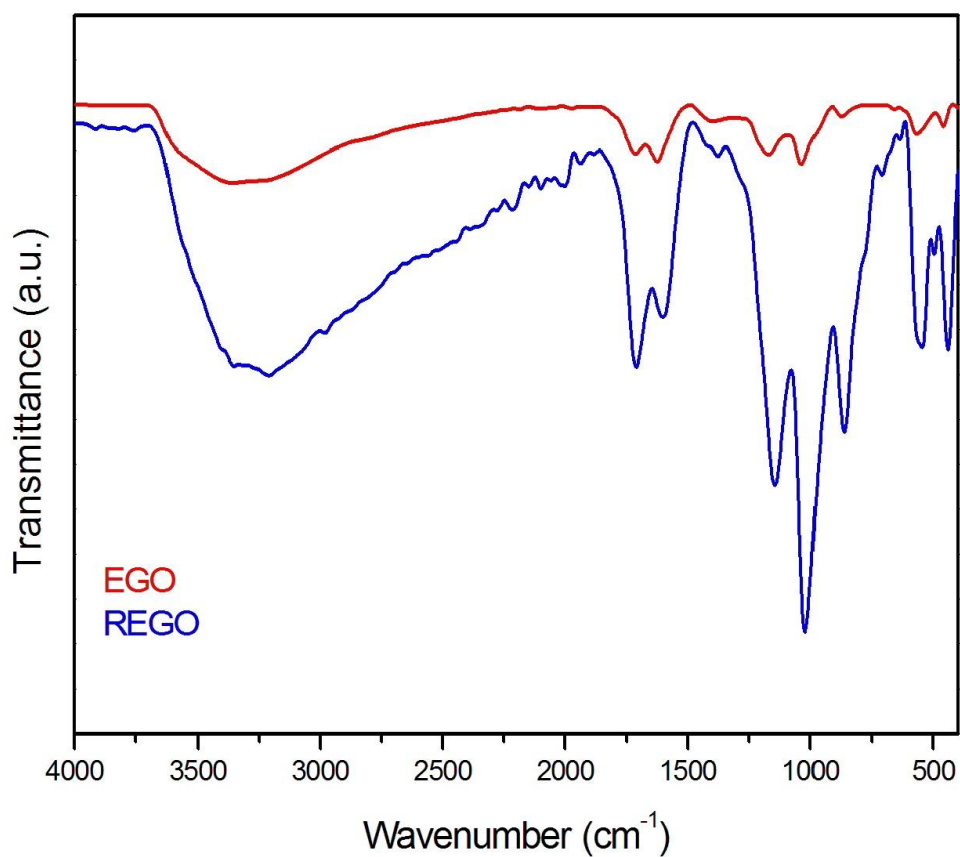


Figure 4.1 FT-IR spectrum of EGO and REGO

Figure 4.1, shows the FTIR spectra of EGO and REGO sheets in the wave number range of 400-4000  $\text{cm}^{-1}$ . As seen, the EGO and REGO exhibited various peaks due to the presence of different types of oxygen functionalities onto the surfaces. The strong peak observed at 3400  $\text{cm}^{-1}$  corresponds to the stretching vibration of O-H. Peaks observed at 1710 and 1614  $\text{cm}^{-1}$  belong to the stretching vibration of C=O and the skeletal vibration of unoxidized graphitic domains (aromatic C=C), respectively. Furthermore, the characteristic peaks observed at the wave numbers of 1392, 1150, 1035 and 870  $\text{cm}^{-1}$  correspond to the stretching of C-O, asymmetric and symmetric stretching of carbonyl groups  $-\text{CO}_2$  and stretching of C-O bonds, respectively. It can be seen in the figure that the stretching vibration of O-H at the wave number of 3400  $\text{cm}^{-1}$  and the stretching vibrations of C=O at the wave number of 1710  $\text{cm}^{-1}$  were still observed in the REGO. But, these peaks were smaller than those observed in the FTIR spectra of EGO. These results pointed out the chemical reduction of EGO with the hydrazine hydride were significantly reduced by the oxygen species but some carboxyl groups were even remained onto the sheets (Durmus et al., 2015).

#### 4.1.1.1.2 Reduced Expanded Graphene Oxide- Gold (REGO-Au)

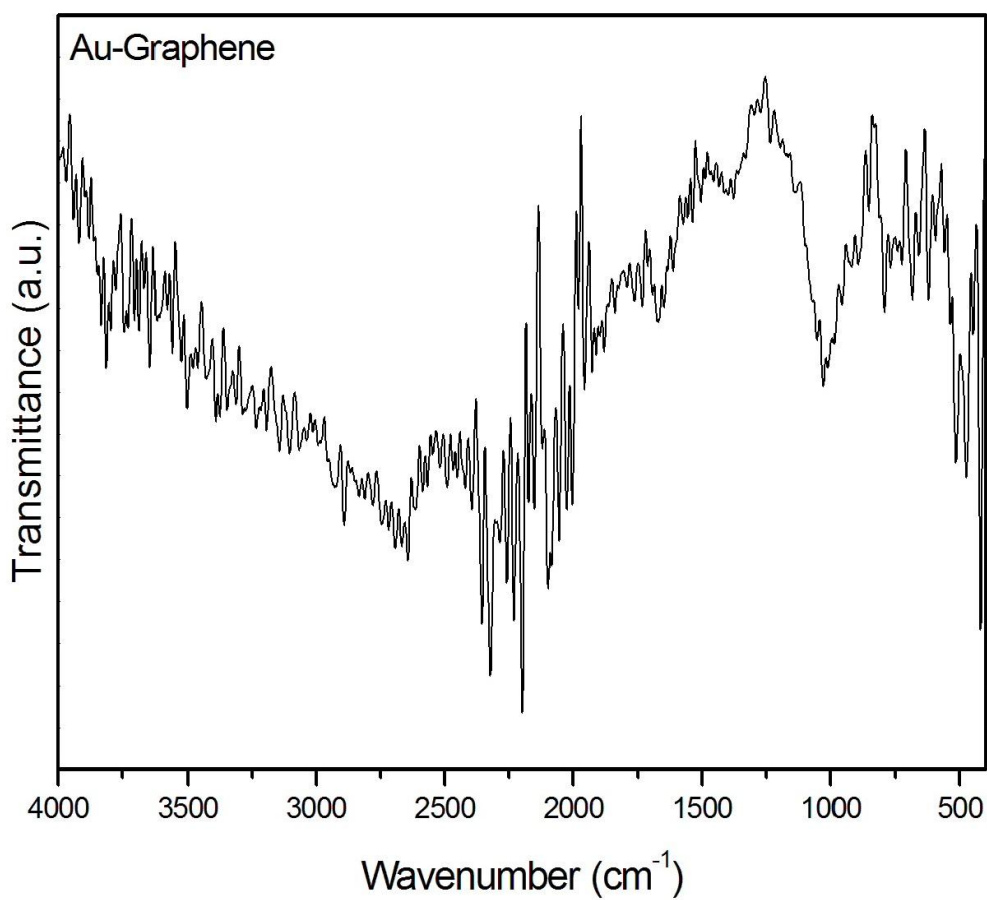


Figure 4.2 FT-IR spectrum of REGO-Au.

FTIR spectra of EGO and REGO sheets in the wave number range of 400-4000  $\text{cm}^{-1}$ , which can be seen in figure 4.2 The REGO-Au exhibited various peaks due to the presence of different types of oxygen functionalities onto the surfaces.

#### 4.1.1.1.3 Reduced Expanded Graphene Oxide-Palladium (REGO-Pd)

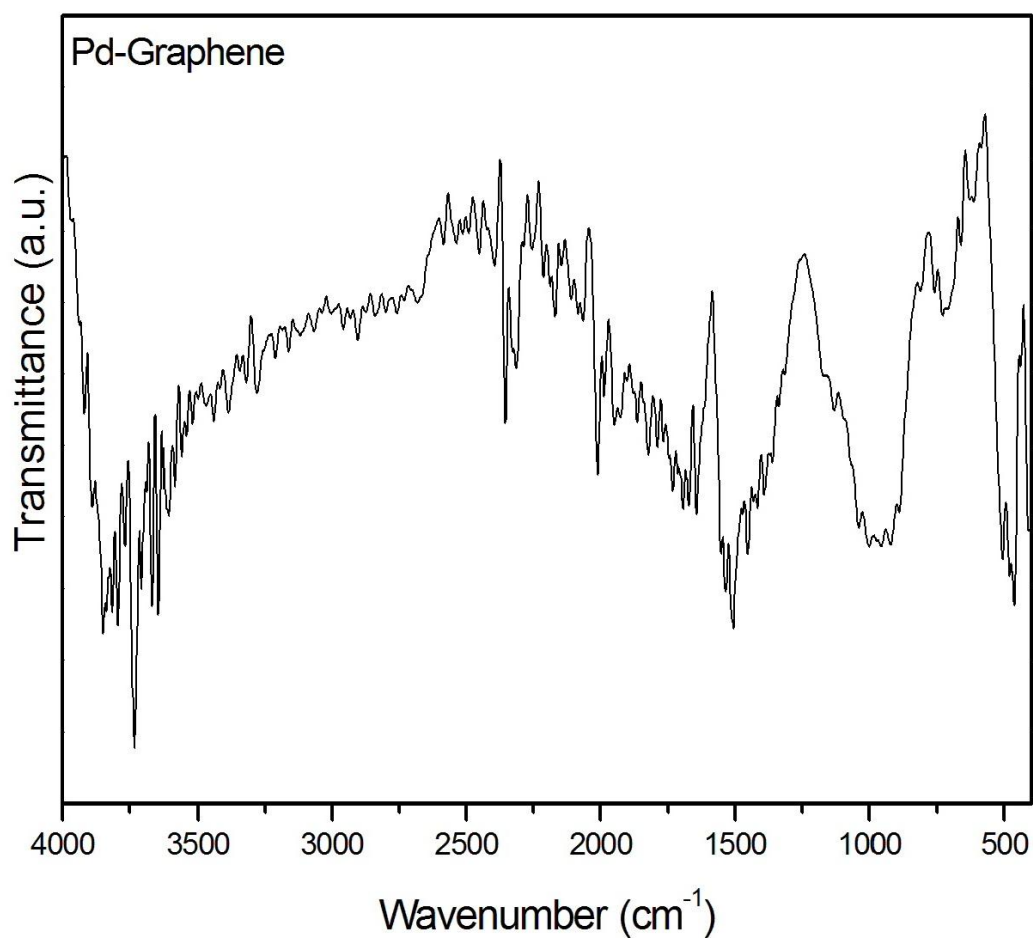


Figure 4.3 FT-IR spectrum of REGO-Pd.

FTIR spectra of REGO-Pd sheets in the wave number range of 500-4000 cm<sup>-1</sup>, can be seen in the figure 4.3 The REGO-Pd exhibited various peaks due to the presence of different types of oxygen functionalities onto the surfaces.

#### 4.1.1.1.4 Reduced Expanded Graphene Oxide- Platinum (REGO-Pt)

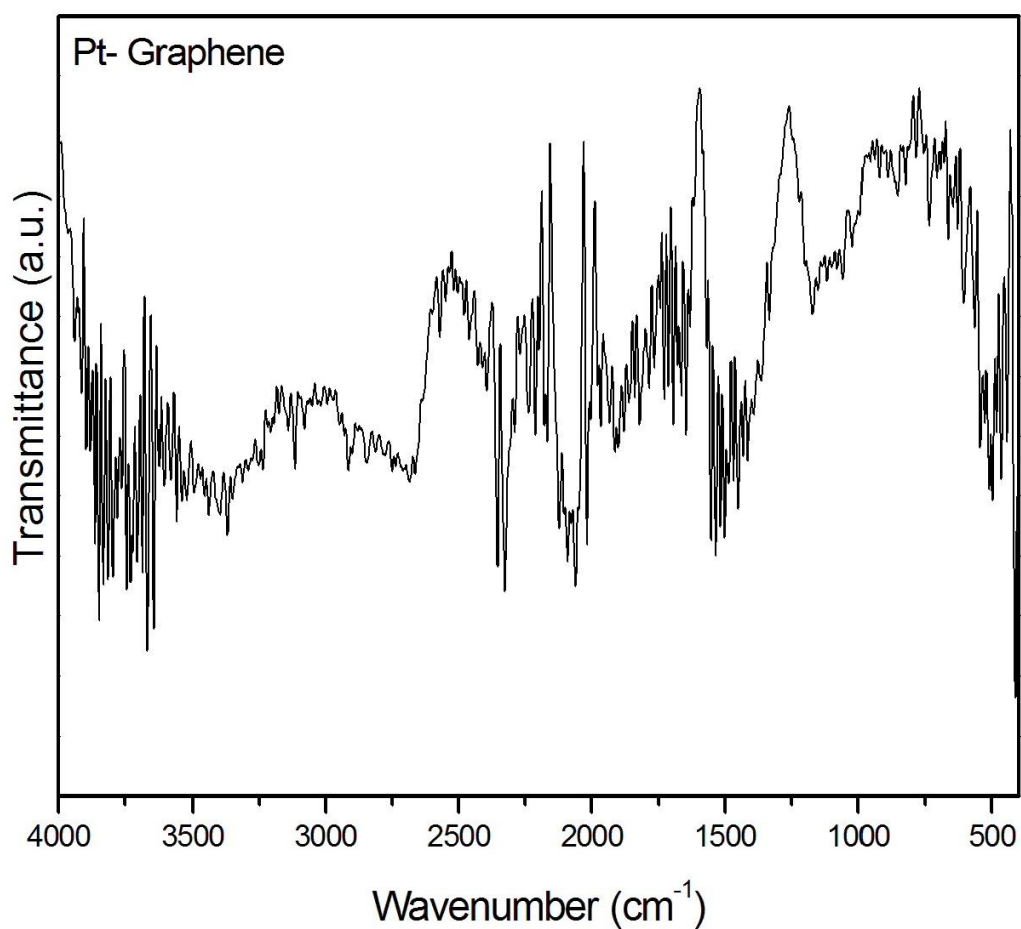


Figure 4.4 FT-IR spectrum of REGO-Pt.

FTIR spectra of REGO-Pt sheets in the wave number range of 500-4000 cm<sup>-1</sup>, which is demonstrated in figure 4.4 The REGO-Pt exhibited various peaks due to the presence of different types of oxygen functionalities onto the surfaces.

#### 4.1.1.2 RAMAN Analysis of EG, EGO and REGO

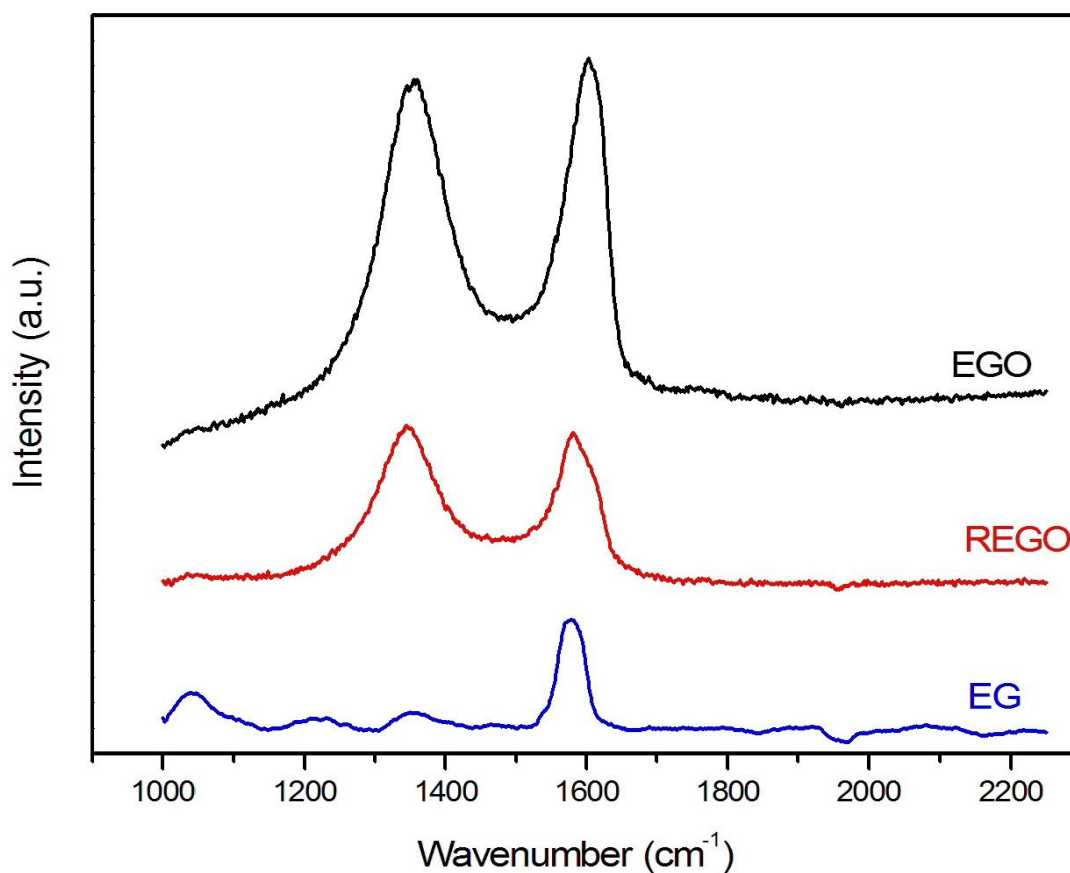


Figure 4.5 RAMAN spectrums of EG, EGO and REGO

The Raman spectra of EG, EGO and REGO are given in Figure 4.5 EG exhibits a sharp *G* band at 1580 cm<sup>-1</sup> and a weak *D* band while the EGO displays two distinct peaks at 1356 and 1602 cm<sup>-1</sup>. The *G* and *D* bands are attributed to the graphitic crystal lattice vibration and defects and disorders in graphitic crystal lattices in the carbon materials, respectively. It was also found that the REGO shows less intense but clear *D* and *G* bands at 1345 and 1584 cm<sup>-1</sup> (Durmus et al., 2015).

#### 4.1.1.3 UV Analysis of EG, EGO and REGO

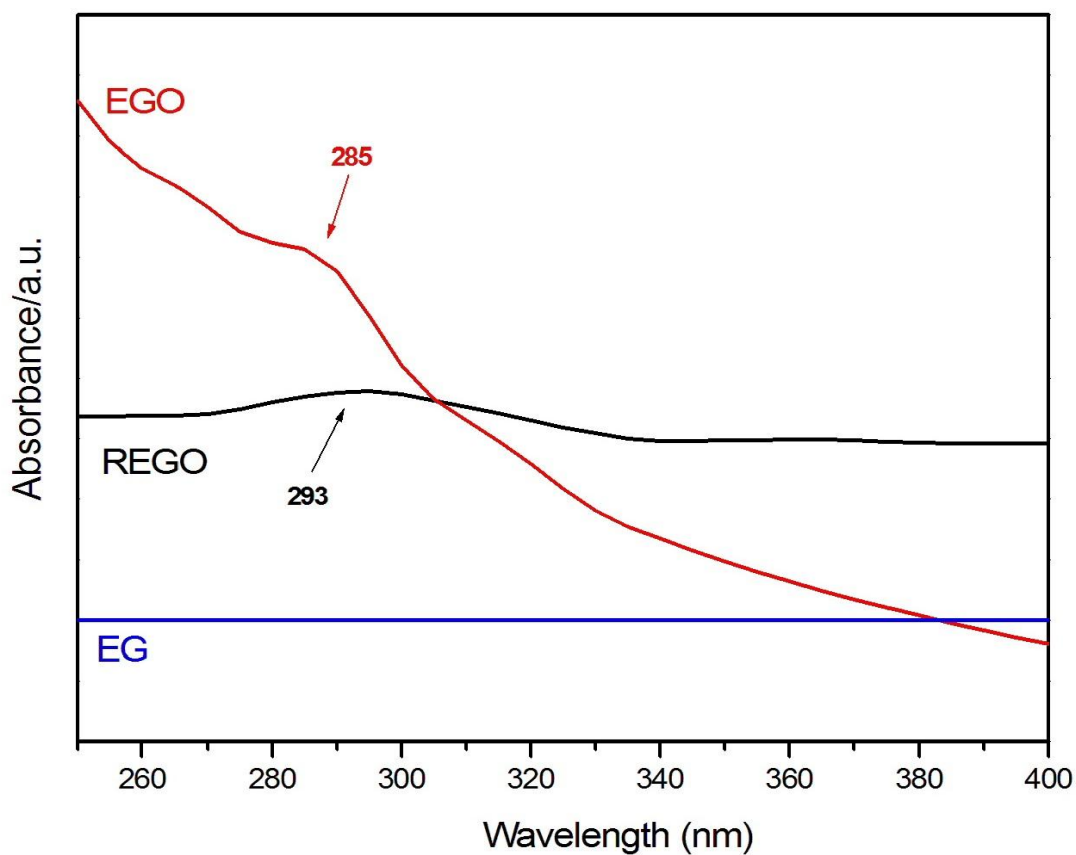


Figure 4.6 UV analysis of EG, EGO and REGO

Figure 4.6, shows the ultraviolet-visible (UV) absorption spectra of spectra of EG, EGO and REGO sheets in the wave number range of 250-400  $\text{cm}^{-1}$ . For pure EGO, peak at about 227 nm and a shoulder at around 290 nm are assigned to the pi to anti-pi ( $\pi \rightarrow \pi^*$ ) transition of the aromatic carbon-carbon bonds and the n to anti-pi ( $n \rightarrow \pi^*$ ) transitions of the carbon = oxygen bonds respectively. For REGO, a peak at 293 nm indicates the characteristic of graphene and is attributed to the aromatic carbon = carbon bonds.

#### 4.1.1.4 X-ray powder diffraction (XRD)

##### 4.1.1.4.1 Reduced Expanded Graphene Oxide(REGO)

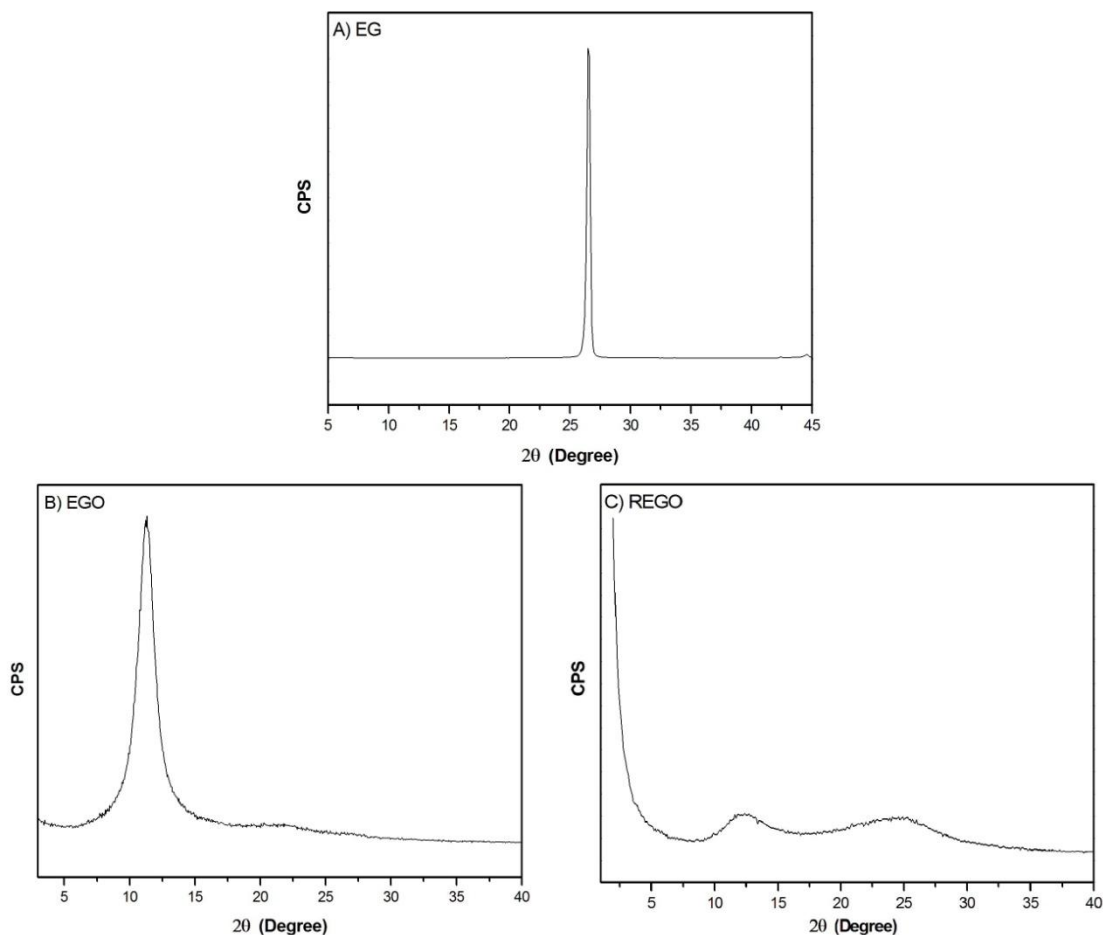


Figure 4.7 XRD patterns of A) EG, B) EGO and C) REGO

Figure 4.7 shows the XRD patterns of EG, EGO and REGO. EG exhibits a characteristic sharp and intense peak at the diffraction angle of  $26.5^\circ$  which corresponds to the  $d_{001}$  planes of graphite. The inter-gallery distance between the graphite sheets was calculated to be 0.336 nm for the EG by the Bragg's equation. As clearly seen in the figure, the  $d_{001}$  peak shifted to the lower diffraction angle at  $2\theta=11.3^\circ$  which corresponds to inter-gallery distance of 0.782 nm for the EGO. REGO exhibited two

broad peaks at the diffraction angles of  $12.2^\circ$  and  $24.8^\circ$  which can be attributed to the  $d_{001}$  and  $d_{002}$  planes of graphene sheets (Dervisevic et al., 2015b).

#### 4.1.1.4.2 Reduced Expanded Graphene Oxide- Gold (REGO-Au)

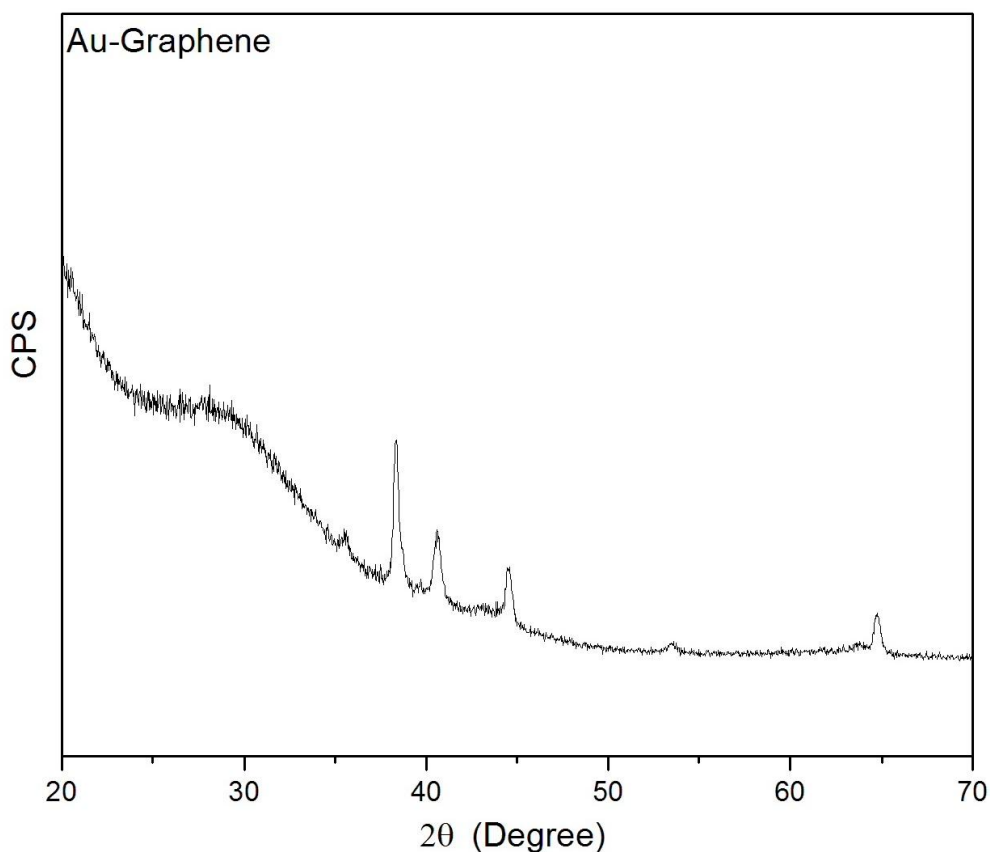


Figure 4.8 XRD patterns of REGO-Au.

XRD spectrums REGO-Au, in which three representative diffraction peaks can be assigned to the (111), (200), and (220) planes of fcc metallic structure (Fenga et al., 2014). A broad peak is observed at about  $25^\circ$  which is indicating that Au synthesized on graphene sheets was successful.

#### 4.1.1.4.3 Reduced Expanded Graphene Oxide- Palladium (REGO-Pd)

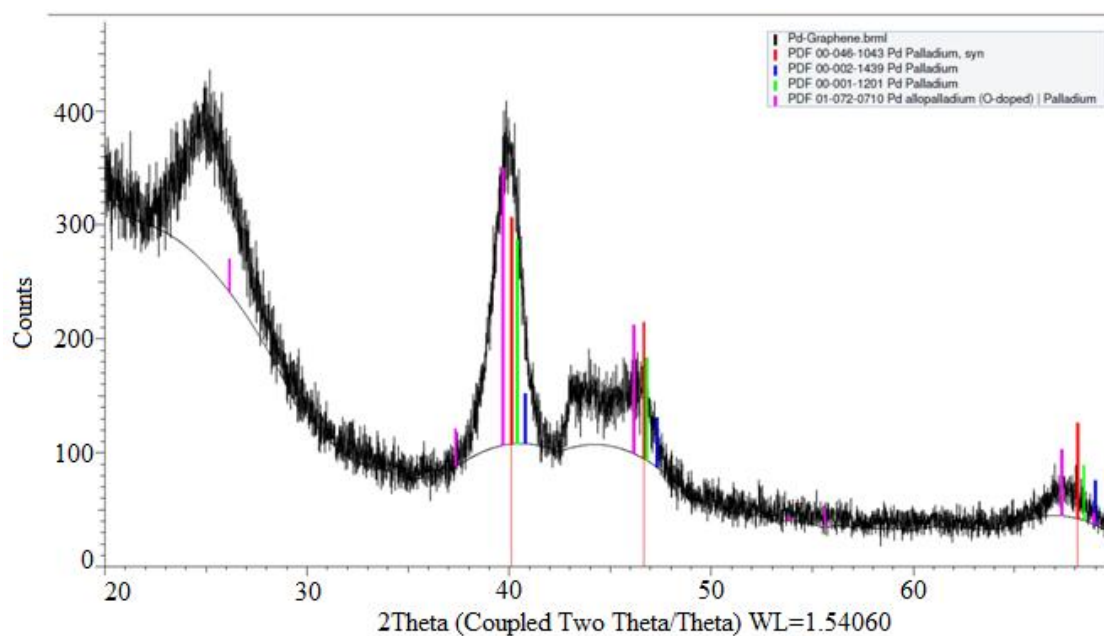


Figure 4.9 XRD patterns of REGO-Pd

XRD spectrums Pd-graphene, in which three representative diffraction peaks can be assigned to the (111), (200), and (220) planes of fcc metallic structure (Fenga et al., 2014). In addition, a broad peak is observed at about 25° graphene for Pd-graphene samples. This observation confirms that platinum successfully was reduced with hydrazine on graphene.

#### 4.1.1.4.4 Reduced Expanded Graphene Oxide- Platinum (REGO-Pt)

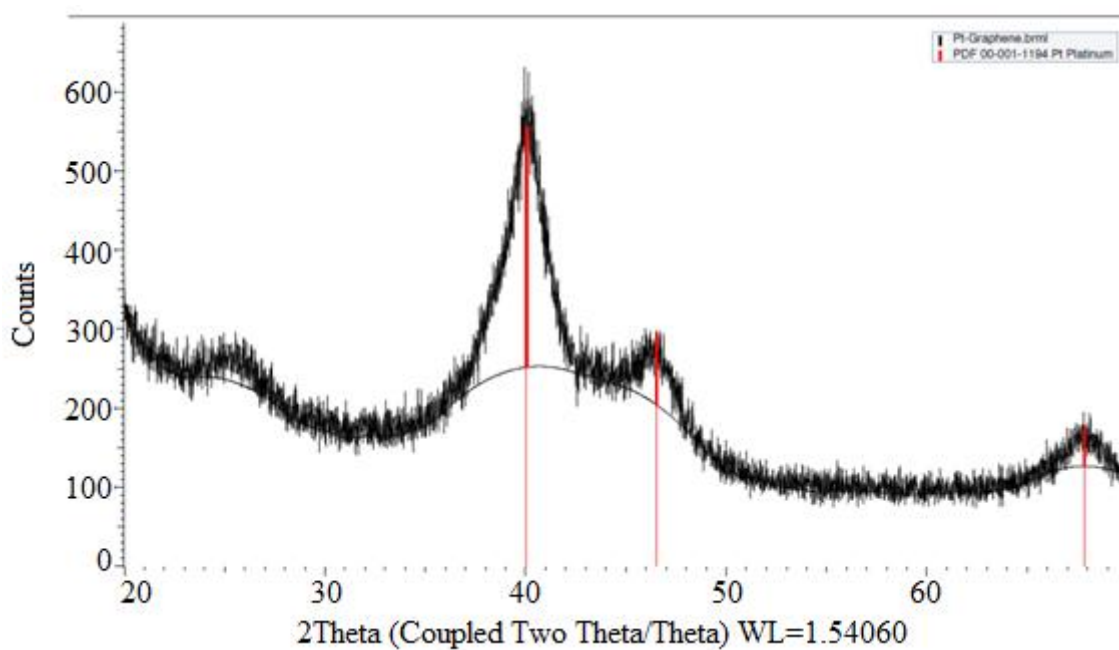


Figure 4.10 XRD patterns of REGO-Pt

XRD spectrums Pt-graphene, in which three representative diffraction peaks can be assigned to the (111), (200), and (220) planes of fcc metallic structure (Fenga et al., 2014). In addition, a broad peak is observed at about 25° graphene for Pt-graphene samples. This observation confirms that platinum successfully was reduced with hydrazine on graphene

## 4.1.2 Electrochemical

### 4.1.2.1 Cyclic Voltammogram

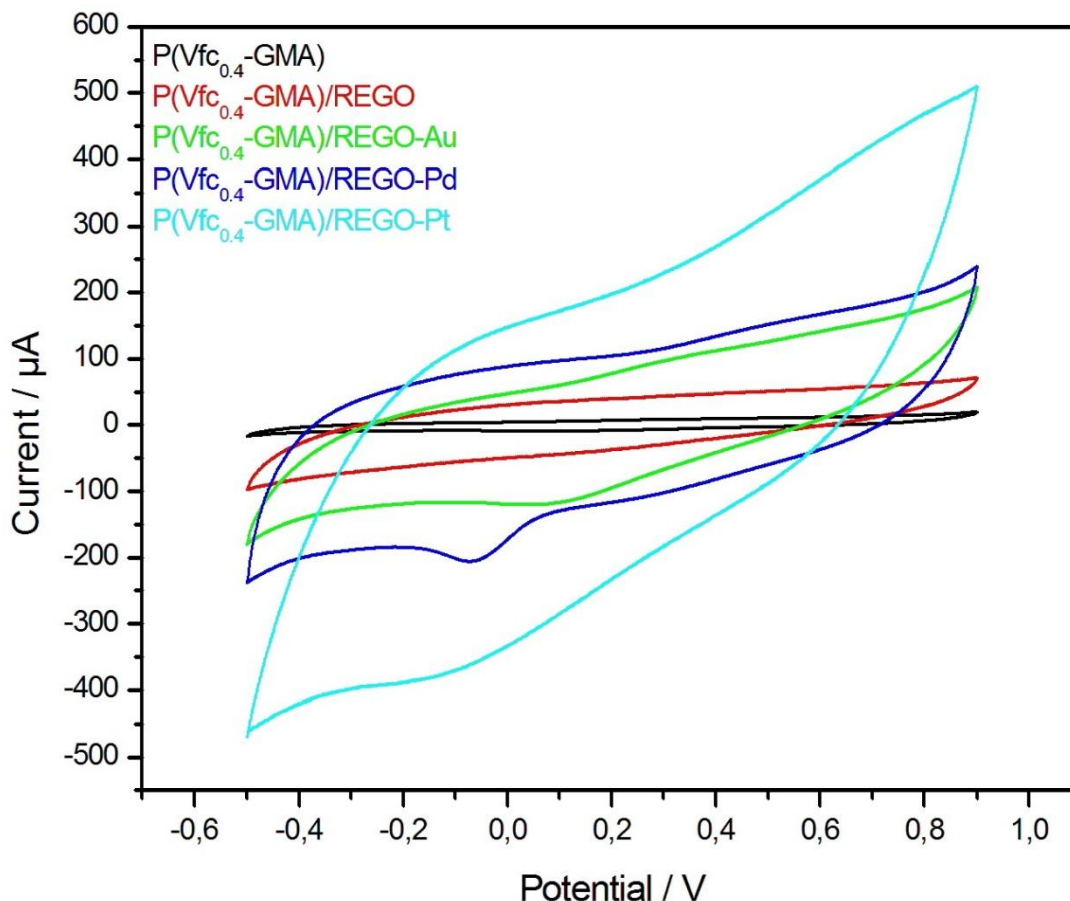


Figure 4.11 Cyclic voltammograms of P(Vfc<sub>0.4</sub>-GMA), P(Vfc<sub>0.4</sub>-GMA)/ REGO, P(Vfc<sub>0.4</sub>-GMA)/ REGO-Au, P(Vfc<sub>0.4</sub>-GMA)/ REGO-Pd and P(Vfc<sub>0.4</sub>-GMA)/ REGO-Pt coated electrodes in 10mM PBS pH 7.0 at scan rate of 50mV<sup>-s</sup>

Cyclic voltammograms of P(Vfc<sub>0.4</sub>-GMA), P(Vfc<sub>0.4</sub>-GMA)/ REGO, P(Vfc<sub>0.4</sub>-GMA)/ REGO-Au, P(Vfc<sub>0.4</sub>-GMA)/ REGO-Pd and P(Vfc<sub>0.4</sub>-GMA)/ REGO-Pt coated electrodes were measured in order to evaluate the effect of the REGO, REGO-Au, REGO-Pd and REGO-Pt and its nano-composite in polymeric mediators film. The ferrocene units of P(Vfc<sub>0.4</sub>-GMA) redox peak current increased with addition of REGO, REGO-Au, REGO-Pd and REGO-Pt (see Figure 4.11) nanocomposite in copolymer solution, respectively. Results indicate that accelerating electron transfer on the electrode surface has been occurred in following sequence: REGO -- REGO-Au --

REGO-Pd -- REGO-Pt. Which REGO-Pt has been shown as most dominant factor in electron transfer acceleration as well it can be characterized as a nano-material which increases the diffusion of the electrons. Applied potential of biosensors of 0.35V was selected due to oxidation and reduction peaks of ferrocene mediator, and by that interference of other molecules was avoided. In order to understand the logic behind the selection of applied potential scan rate of P(Vfc<sub>0.4</sub>-GMA) coated electrode can be observed (see Figure 4.12 A)

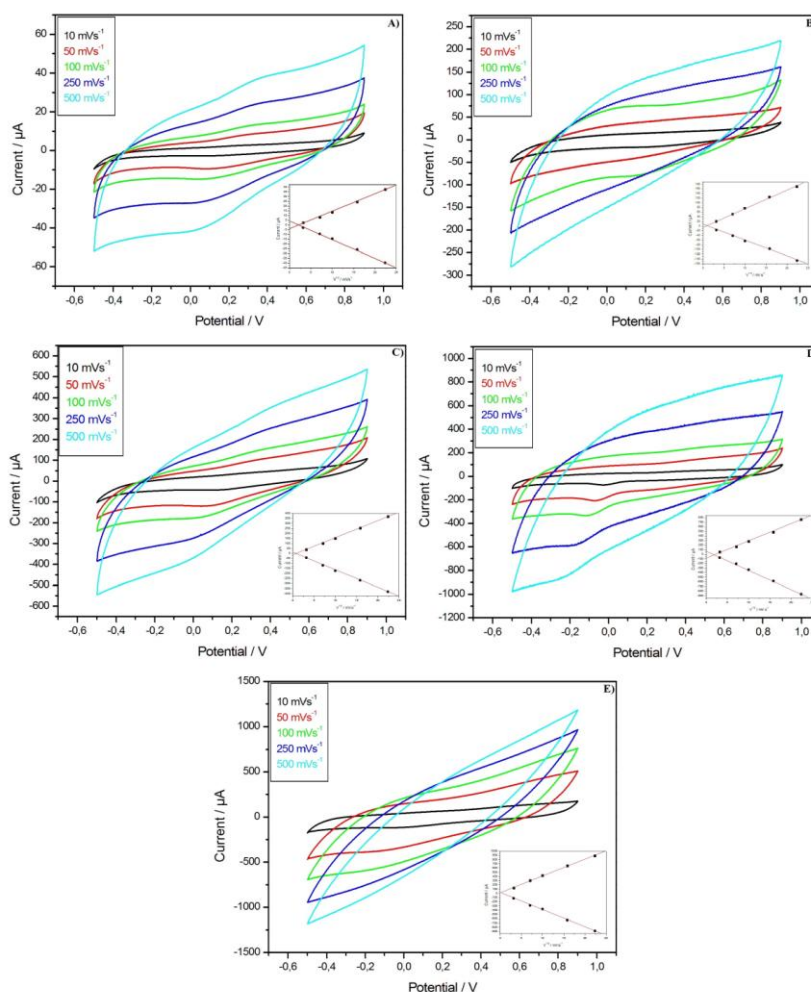


Figure 4.12 Cyclic voltammogram of A) P(Vfc<sub>0.4</sub>-GMA), B) P(Vfc<sub>0.4</sub>-GMA)/ REGO, C) P(Vfc<sub>0.4</sub>-GMA)/ REGO-Au, D) P(Vfc<sub>0.4</sub>-GMA)/ REGO-Pd and E) P(Vfc<sub>0.4</sub>-GMA)/ REGO-Pt coated electrodes with scan rates of 10, 50, 100, 250, 500  $\text{mV}^{-\text{s}}$  in 10mM PBS pH 7.0.

For investigation and characterization of electrochemically active electrodes cyclic voltammogram methods were used to record number of oxidations states as well electron transfer rate behaviors (see Figure 4.12). Results are recorded between scan rates of  $10\text{mVs}^{-1}$  to  $500\text{mVs}^{-1}$  in  $10\text{mM BS pH } 7.0$  in the potential range from  $-0.5\text{V}$  to  $9.0\text{V}$  and the effect of scan rate on the peak current has been obtained ( $I_{pa}$  and  $I_{pc}$ ).  $\text{P(Vfc}_{0.4}\text{-GMA)}$  electrodes anodic peak potential ( $E_{pa}$ ) was recorded at  $0.35\text{V}$  which is related to oxidation of polymer and the cathodic peak potential ( $E_{ps}$ ) obtained at  $0.15\text{V}$  (see Figure 4.12 A). Can be attributed to its reverse processes, as well electrochemical quasi reversible process can be observed that as the scan rate increase peak currents and the difference between the peak potentials are increased. Indication that diffusion controlled redox process during forward scan of  $\text{Fe(II)}$  oxidation to  $\text{Fe(III)}$  and reverse scan reduction of  $\text{Fe(III)}$  at the  $\text{P(Vfc}_{0.4}\text{-GMA)}$  coated electrode can be seen from linear relation between peak currents and scan rate represented by square root of scan rate ( $\text{V}^{1/2}$ ) (see inset of Figure 4.12 A). The rest of the cyclic voltamograms shows relationship between peak currents and scan rates of REGO, REGO-Au, REGO-Pd and REGO-Pt mixed with  $\text{P(Vfc}_{0.4}\text{-GMA)}$ . It was found (looking at the same principle described for  $\text{P(Vfc}_{0.4}\text{-GMA)}$ ) that adding nonmaterial's increases the difference between the reduction and oxidation peak of the polymer in the sequence of REGO (see Figure 4.12 B) – REGO-Au (see Figure 4.12 C) - REGO-Pd (see Figure 4.12 D) - REGO-Pt (see Figure 4.12 E). The maximum peak current was obtained from  $\text{P(Vfc}_{0.4}\text{-GMA)}$ / REGO-Pt modified electrode with respect to the scan rate, which is so high that  $\text{P(Vfc}_{0.4}\text{-GMA)}$  coated electrodes results can be neglected. Each of the nanocomposite have positively enhanced electron transfer rate of redox couples, if peak currents ( $I_{pa}$  and  $I_{pc}$ ) are taken in consideration. However, there might be slight shifting in potentials of anodic and cathodic peaks which might be attributed to the limitation of ion diffusion rate.

#### 4.1.2.2 Electrochemical Impedance Spectra

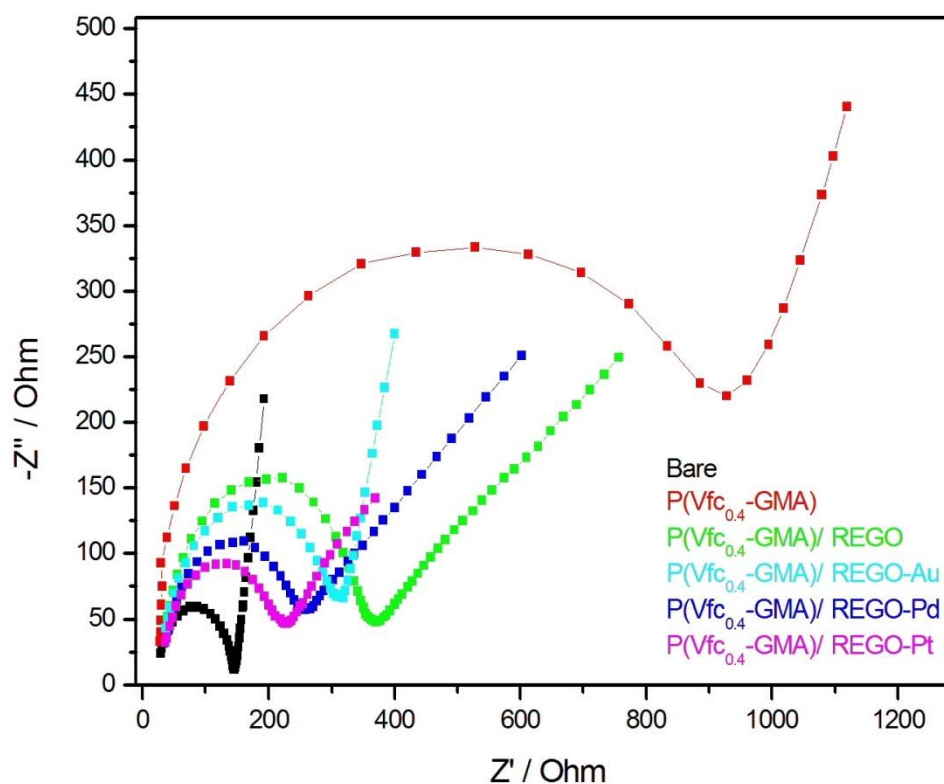


Figure 4.13 Electrochemical Impedance Spectra of bare electrode, P(Vfc<sub>0.4</sub>-GMA), P(Vfc<sub>0.4</sub>-GMA)/ REGO, P(Vfc<sub>0.4</sub>-GMA)/ REGO-Au, P(Vfc<sub>0.4</sub>-GMA)/ REGO-Pd and P(Vfc<sub>0.4</sub>-GMA)/ REGO-Pt coated electrodes in 10mM PBS pH 7.0

Electrochemical impedance spectroscopy (EIS) is used to monitor electron transfer behavior of the modified electrodes surface and in biosensors studies EIS measurements are most commonly represented in Nyquist plot. Nyquist plot is a plot of imaginary part ( $Z''$ ) vs. real part ( $Z'$ ) as a function of frequency which is employed to investigate the charge transfer, as well diameter of semicircle portion of higher frequencies is equal to charge transfer resistance ( $R_{ct}$ ) which is related to electron transfer kinetics of the redox probe at the electrode interface (Devi et al., 2013a). EIS measurements of bare electrode, P(Vfc<sub>0.4</sub>-GMA), P(Vfc<sub>0.4</sub>-GMA)/ REGO, P(Vfc<sub>0.4</sub>-GMA)/ REGO-Au, P(Vfc<sub>0.4</sub>-GMA)/ REGO-Pd and P(Vfc<sub>0.4</sub>-GMA)/ REGO-Pt coated electrodes were conducted in order see charge transfer behavior of co-polymer

nanocomposite based biosensors (see Figure 4.13). Charge transfer resistance for proposed electrodes has been summarized (see Table 4.1). Results are demonstrating that charge transfer resistance has been increased from 116  $\Omega$  to 863  $\Omega$  when bare electrode has coated with P(VFc<sub>0.4</sub>-GMA) which can be attributed to fact that polymeric mediator is poor charge conductor at low frequencies and causes hindrance to electron transfer. However, when P(VFc<sub>0.4</sub>-GMA) has been modified with REGO, REGO-Au, REGO-Pd and REGO-Pt Rct has been decreased to 189  $\Omega$  which is close result to bare PGE electrode and suggesting that among all nanocomposites REGO-Pt can decrease resistance of the coated electrode as well hold high electron transfer efficiency.

Table 4.1 R<sub>ct</sub> values of modified electrodes with different bionanocomposite

Electrode	R <sub>ct</sub> ( $\Omega$ )
Bare (PGE)	116
poly(VFc <sub>0.4</sub> -GMA)	863
poly(VFc <sub>0.4</sub> -GMA)/REGO	323
poly(VFc <sub>0.4</sub> -GMA)/REGO-Au	272
poly(VFc <sub>0.4</sub> -GMA)/REGO-Pd	215
poly(VFc <sub>0.4</sub> -GMA)/REGO-Pt	189

### 4.1.3 Morphological properties

#### 4.1.3.1 SEM Analyses

##### 4.1.3.1.1 EG, EGO and REGO

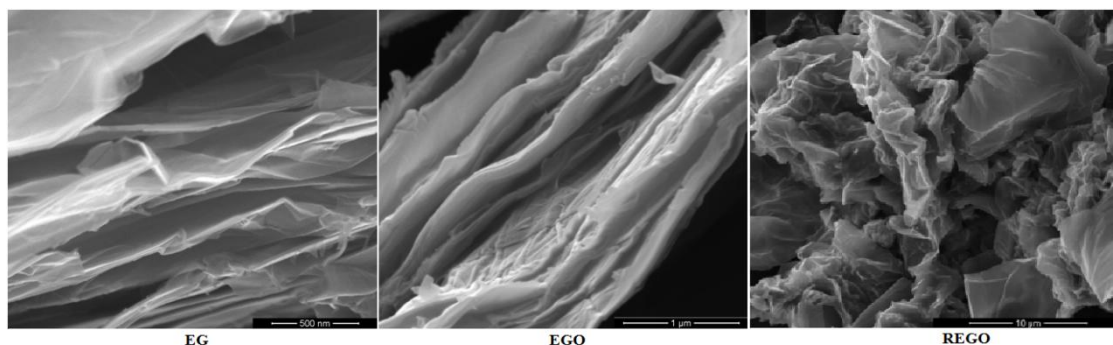


Figure 4.14 SEM analyses of EG, EGO and REGO

SEM micrographs of EG, EGO, and REGO were recorded respectively. Highly porous and layered structure of commercial EG having large stacks, possibly consisting of hundreds of graphene nano-sheets, can be clearly seen (see Figure 4.14). The mean size of graphitic nano-sheets was not disrupted with the oxidation, but the surface properties of modified product were strongly affected. As seen in the figure 4.14, the surfaces of EGO nano-sheets are rough, and the edges are highly crumpled. On the other hand, after strong reduction the SEM image REGO clearly signifies that the very thin, wrinkled, loose open and transparent graphene sheets obtained by the chemical reduction process (Durmus et al., 2015).

#### 4.1.3.1.1 REGO-Au, REGO-Pd and REGO-Pt

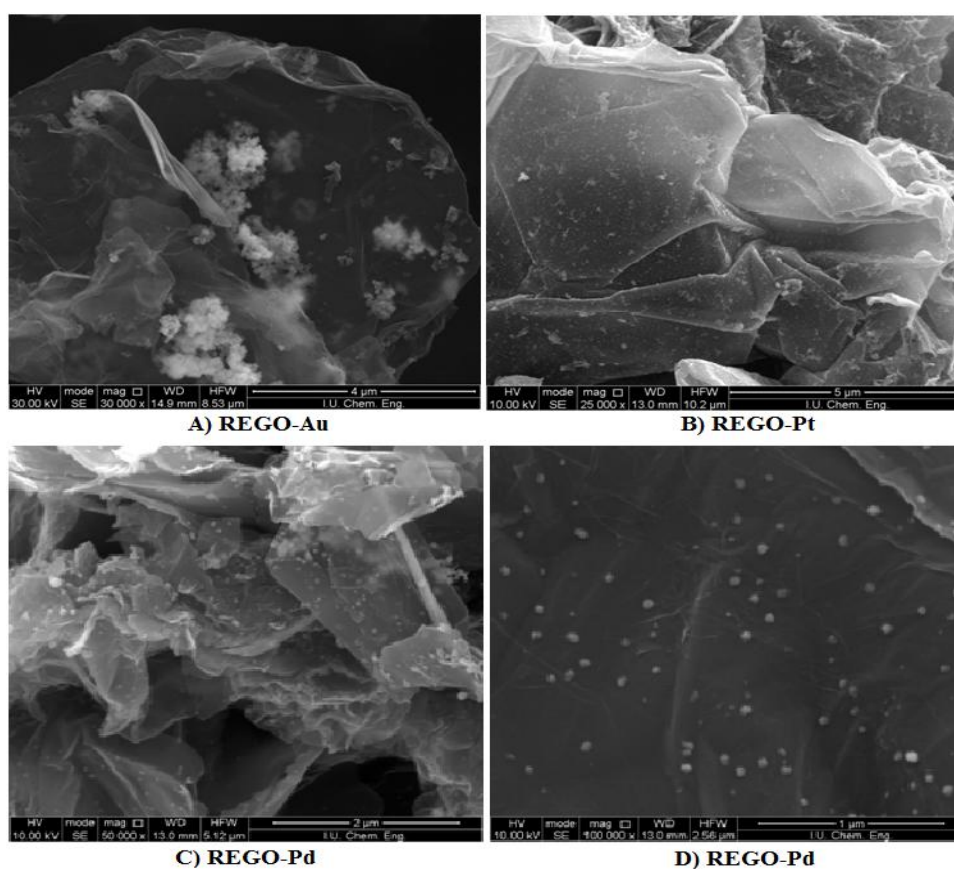


Figure 4.15 SEM analyses of A) REGO-Au, B) REGO-Pt, C) REGO-Pd and D) REGO-Pd

SEM images of REGO, REGO-Au, REGO-Pd and REGO-Pt clearly signify that the very thin, wrinkled, loose open and transparent graphene sheets obtained by the chemical reduction process are modified with Gold, Palladium and Platinum (see Figure 4.15)

### 4.1.3.2 TEM Analyses

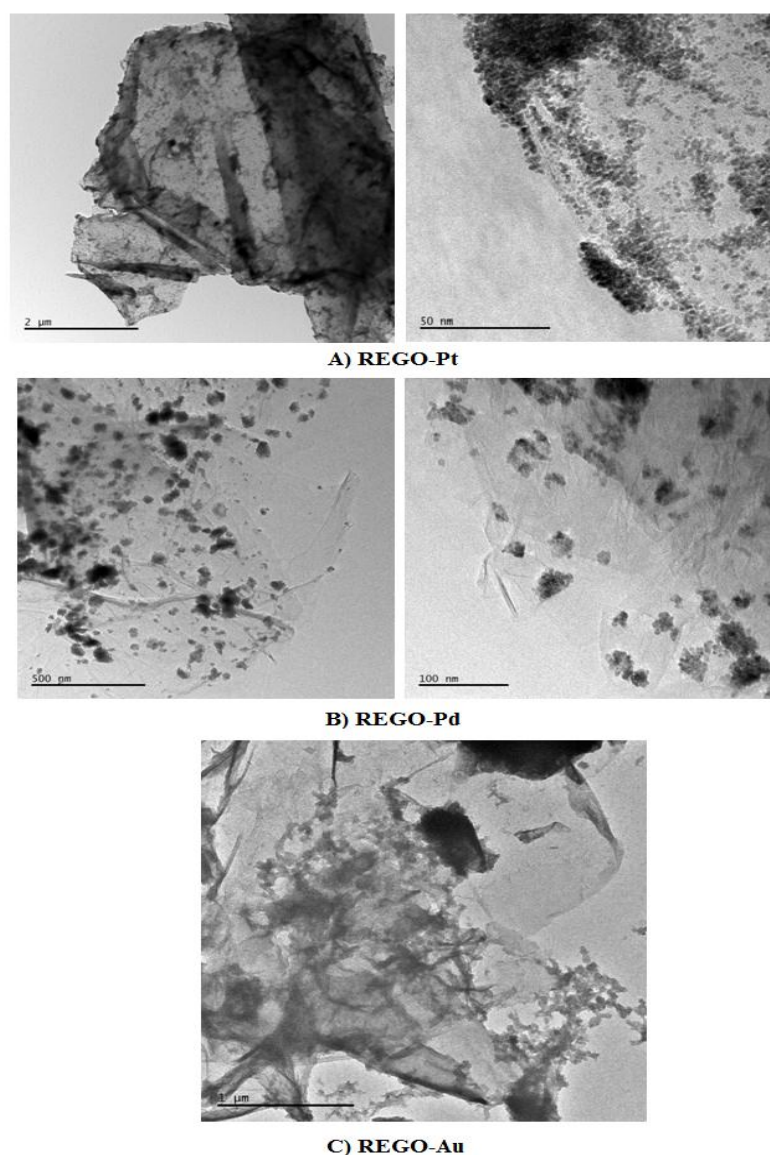


Figure 4.16 TEM analyses of A) REGO-Pt, B) REGO-Pd and C) REGO-Au

TEM images of REGO-Pt, REGO-Pd and REGO-Au represent expanded graphite composed of nano-thick graphene layers modified with Gold, Platinum and Palladium. Some wrinkled parts of graphene layers can also be seen especially close to the edges and the lateral size of graphene sheets can be estimated to be larger than a few microns which means that an extremely high surface area can be accessible for the

chemically treated EG sheets, the aspect ratio of REGO is probably much higher than that of EG, and clearly it can be seen Pt, Pd, Au modified.

## 4.2 DETERMINATION OF EXPERIMENTAL VARIABLES

### 4.2.1 Optimum pH

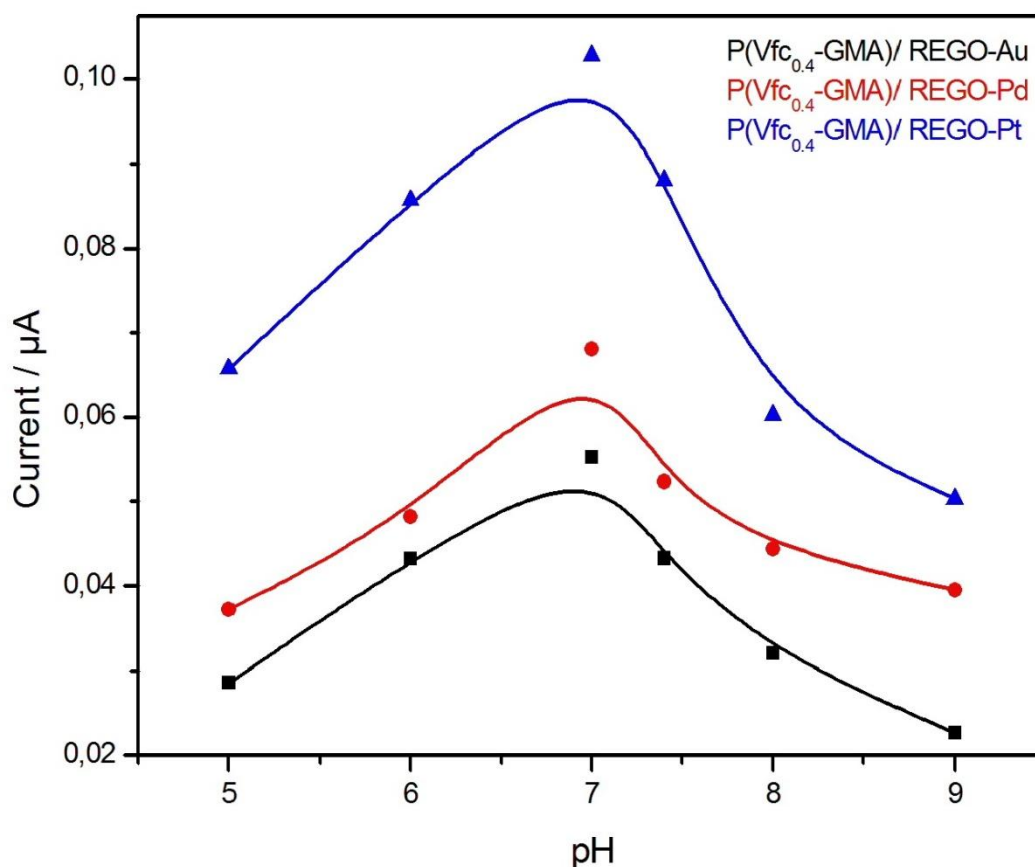


Figure 4.17 The effect of buffer pH on the response of P(Vfc<sub>0.4</sub>-GMA)/ REGO-Au, P(Vfc<sub>0.4</sub>-GMA)/ REGO-Pd and P(Vfc<sub>0.4</sub>-GMA)/ REGO-Pt fabricated electrodes on xanthine addition (10mM PBS, +0.35V applied potential)

Dependence of fabricated enzyme electrode on pH, was investigated over the range of pH 5.0 to 9.0 10mM PBS in the presence of 5μM xanthine substrate. The maximum amperometric current response of P(Vfc<sub>0.4</sub>-GMA)/ REGO-Au, P(Vfc<sub>0.4</sub>-GMA)/ REGO-Pd and P(Vfc<sub>0.4</sub>-GMA)/ REGO-Pt based xanthine electrode was found to be at pH 7.0 (see Figure 4.17). Obtained results indicates that the immobilization technique has no big influence on the optimum pH of Xanthine Oxidase, as well as

obtained maximum amperometric response of xanthine biosensors at pH 7.00 has been reported in the literature (Dervisevic et al., 2015a, Dalkiran et al., 2014, Devi et al., 2012b, Devi et al., 2011). As seen in figure 4.17 pH lower than 5.00 would deactivate enzyme and biosensors would provide very small current response, this might be due to acidic medium since it deforms enzyme and leads to loss of its catalytic capability. Biosensor showed increment of current response by increasing pH until it reaches its maximum plateau at pH 7.00, further increase of pH results in gradual decrement in biosensor response. However it is clearly seen that P(Vfc<sub>0.4</sub>-GMA)/ REGO-Pt based electrode had almost double response as compared to P(Vfc<sub>0.4</sub>-GMA)/ REGO-Au and P(Vfc<sub>0.4</sub>-GMA)/ REGO-Pd based electrodes. Therefore, pH 7.0 PBS was selected as the working pH in further experiments.

### 4.2.2 Optimum Temperature

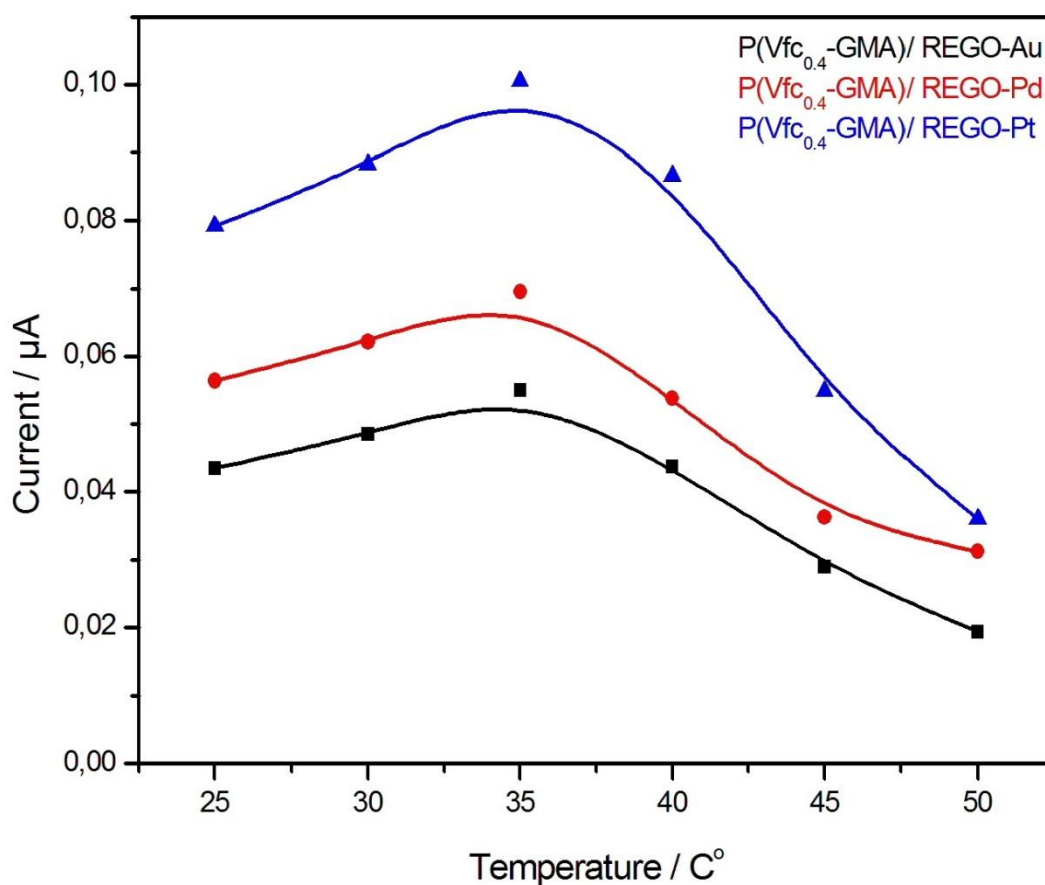


Figure 4.18 Temperature effect on amperometric response of P(Vfc<sub>0.4</sub>-GMA)/ REGO-Au, P(Vfc<sub>0.4</sub>-GMA)/ REGO-Pd and P(Vfc<sub>0.4</sub>-GMA)/ REGO-Pt electrodes on known amount of xanthine (10mM PBS pH 7.0, +0.35V applied potential)

The temperature effect on the electrochemical response of the electrode was studied across a range of 25°C to 50°C. The amperometric current response of P(Vfc<sub>0.4</sub>-GMA)/ REGO-Au, P(Vfc<sub>0.4</sub>-GMA)/ REGO-Pd and P(Vfc<sub>0.4</sub>-GMA)/ REGO-Pt electrodes was gradually increasing from 25°C to 35°C after which response drastically decreases at higher temperatures (see Figure 4.18). Amperometric current response decrease at higher temperatures might occur because of decrement of molecular oxygen in solution or because of thermal deactivation of enzyme (Pei and Li, 2000). The optimum temperature was 35°C was for all three electrodes. However P(Vfc<sub>0.4</sub>-GMA)/ REGO-Pt in comparison with electrodes P(Vfc<sub>0.4</sub>-GMA)/ REGO-Au and P(Vfc<sub>0.4</sub>-

GMA)/ REGO-Pd had almost two times higher current response value. As well, it can be concluded that heat resistance of Xanthine oxidase has not been changed by the immobilization technique as reported by Dervisevic et al., (Dervisevic et al., 2015b).

#### 4.3 AMPEROMETRIC RESPONSE OF BIONANOCOMPOSITE ELECTRODES

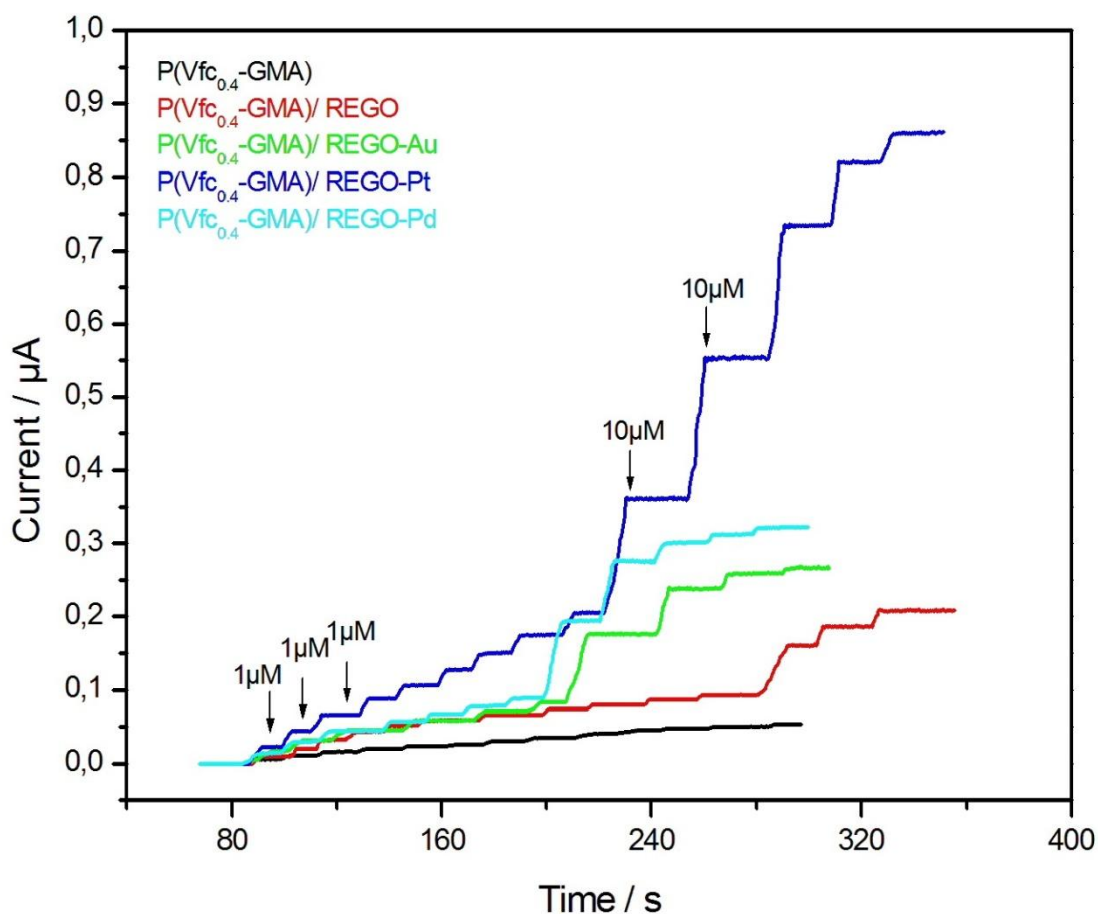


Figure 4.19 Amperometric response of P(Vfc<sub>0.4</sub>-GMA), P(Vfc<sub>0.4</sub>-GMA)/ REGO, P(Vfc<sub>0.4</sub>-GMA)/ REGO-Au, P(Vfc<sub>0.4</sub>-GMA)/ REGO-Pt and P(Vfc<sub>0.4</sub>-GMA)/ REGO-Pd electrodes to successive addition of 1  $\mu\text{M}$  and 10  $\mu\text{M}$  xanthine in stirred 10mM PBS, pH 7.0 at room temperature and applied potential of 0.35V

Comparison of amperometric responses of Xanthine Oxidase immobilized on to P(Vfc<sub>0.4</sub>-GMA), P(Vfc<sub>0.4</sub>-GMA)/ REGO, P(Vfc<sub>0.4</sub>-GMA)/ REGO-Au, P(Vfc<sub>0.4</sub>-GMA)/ REGO-Pt and P(Vfc<sub>0.4</sub>-GMA)/ REGO-Pd coated electrodes after addition of xanthine aliquots can be seen in figure 4.19. Obtained results indicate that using nanocomposites dramatically increase current response when compared only to electrode which is only coated with P(Vfc<sub>0.4</sub>-GMA). On the other hand, looking at the best response among nanocomposite electrodes P(Vfc<sub>0.4</sub>-GMA)/ REGO-Pt electrode gave the highest amperometric response while P(Vfc<sub>0.4</sub>-GMA)/ REGO-Au and P(Vfc<sub>0.4</sub>-GMA)/ REGO-Pd coated electrode gave quite similar results to each other. P(Vfc<sub>0.4</sub>-GMA)/ REGO-Pt coated electrode which gave best results responded very rapidly producing steady-state current within 2s. Additions were performed by adding 1 $\mu$ M xanthine consequently after was observed constant response and in order to save time and to show efficiency of proposed biosensor 10 $\mu$ M additions of xanthine were applied. It can be observed that response is gradually decreasing after which experiments has been stopped. Decrease in response might be due to big concentration of substrate in electrochemical cell, which after a point started to act as an inhibitor and decrease of enzymes catalytic activity. Further comparison of different electrochemical biosensors analytical performance reported in literature (see Table 4.2) shows that proposed enzyme electrode much better results in response time (RT), detection limit (DL), linear range (LR) and sensitivity, than those biosensors previously reported in literature. Although studies reported in literature shows impressive results they fail to provide parameters good enough for detection of xanthine in early stage.

Table 4.2 Comparison of analytical performance of proposed xanthine biosensor with biosensors in literature

Electrode	RT(s)	DL( $\mu\text{M}$ )	LR( $\mu\text{M}$ )	Sensitivity	Reference
XO/Co <sub>3</sub> O <sub>4</sub> /MWCNT/CS/GCE	5	0.2	0.2 to 16	--	Dalkiran et al. (2014)
P(GMA-co-VFc)/REGO-Fe <sub>3</sub> O <sub>4</sub>	3	0.17	2 to 36	0.17 $\mu\text{A}/\text{M}$	Dervisevic et al. (2015b)
XOD/CHT/Pt/PANI/Fe <sub>3</sub> O <sub>4</sub> NPs/CPE	8	0.10	0.2 to 36	1.0 $\mu\text{A}/\text{M}$	Sadeghi et al. (2014)
XOD/AgNPs/l-Cys/Au	5	0.15	2 to 16	0.2 $\mu\text{A}/\mu\text{M cm}^{-2}$	Devi et al. (2013b)
Modified graphite/gelatin	120	4.5	0 to 40	0.210 $\mu\text{A}/\mu\text{M}$	Dimcheva et al. (2002)
XO/ZnO-NPs-PPy/Pt	5	0.8	0.8 to 40	--	Devi et al. (2011)
PPy-Fc/XO	no	4.5	5 to 20	--	Lawal and Adeloju (2012)
P(VFc <sub>0.4</sub> -GMA)/REGO-Pt	2	0.003	1 to 40	21.98 $\mu\text{A}/\mu\text{M}$	This work

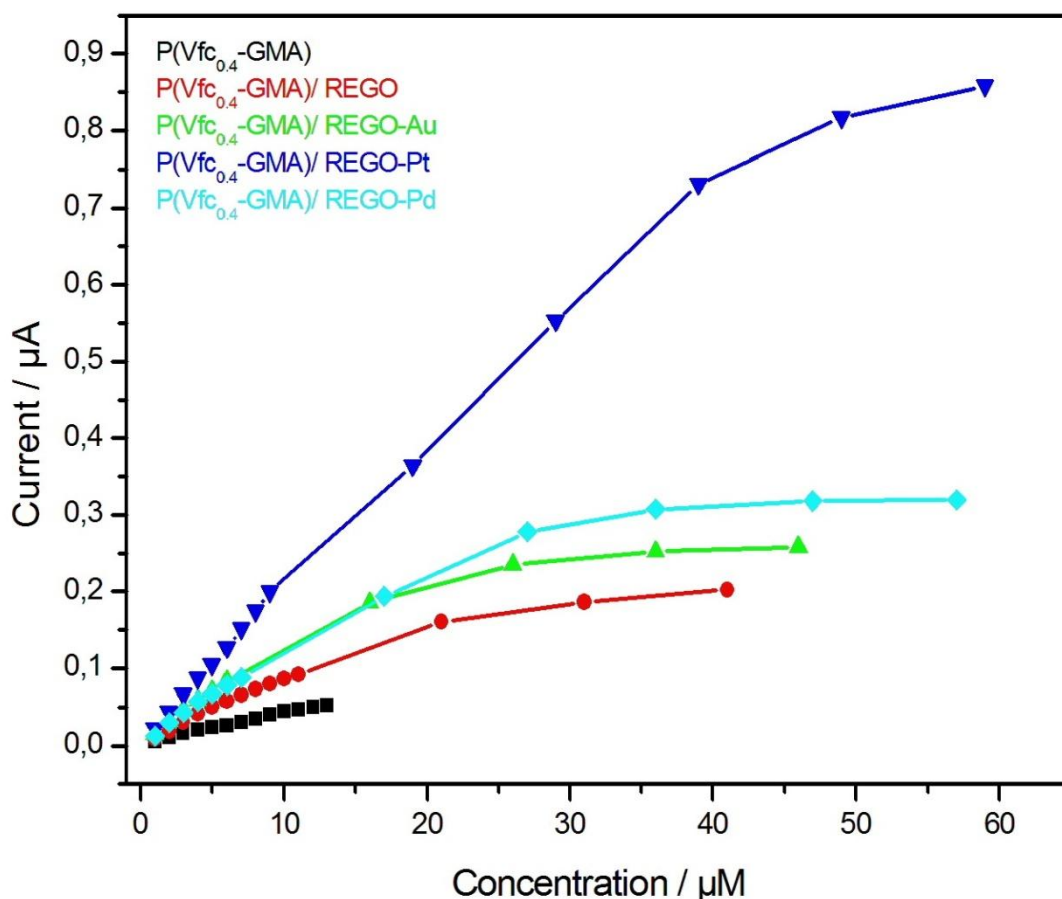


Figure 4.20 Calibration curves for the amperometric response of P(Vfc<sub>0.4</sub>-GMA), P(Vfc<sub>0.4</sub>-GMA)/ REGO, P(Vfc<sub>0.4</sub>-GMA)/ REGO-Au, P(Vfc<sub>0.4</sub>-GMA)/ REGO-Pt and P(Vfc<sub>0.4</sub>-GMA)/ REGO-Pd electrodes

Electrode responded rapidly on xanthine substrate reaching steady-state current within 2 to 4s. Resulting standard calibration plot of P(Vfc<sub>0.4</sub>-GMA)/ REGO-Pt electrode for xanthine over the concentration range from 1 to 40  $\mu\text{M}$  with a correlation coefficient of 0.9985, as well standard calibration plots have been drawn for the other electrode used (see Figure 4.20). Results obtained can be attributed to synergistic influence of nanocomposite polymeric mediators REGO, REGO-Au, REGO-Pd and REGO-Pt which enhances electro-catalytic transfer and increases electron transfer rate due to its large surface area. Comparison of analytical performance and biosensors parameters of enzyme electrodes, P(Vfc<sub>0.4</sub>-GMA)/ REGO-Pt coated electrode showed most satisfying results (see Table 4.3)

Table 4.3 Comparison of analytical performance of proposed xanthine biosensors

<b>Electrode</b>	<b>DL(<math>\mu\text{M}</math>)</b>	<b>Sensitivity (<math>\mu\text{A}/\mu\text{M}</math>)</b>	<b>LR(<math>\mu\text{M}</math>)</b>	<b>RT(s)</b>	<b>R<sup>2</sup></b>
P(VFc <sub>0.4</sub> -GMA)	0.75	4.8	1-10	4	0.9939
P(VFc <sub>0.4</sub> -GMA)/REGO	0.11	10.85	1-20	3	0.9982
P(VFc <sub>0.4</sub> -GMA)/REGO-Au	0.017	13.4	1-20	4	0.9938
P(VFc <sub>0.4</sub> -GMA)/REGO-Pd	0.018	14.1	1-30	3	0.9945
P(VFc <sub>0.4</sub> -GMA)/REGO-Pt	0.003	21.98	1-40	2	0.9985

## 4.4 OPERATIONAL AND STORAGE STABILITY

### 4.4.1 Reusability

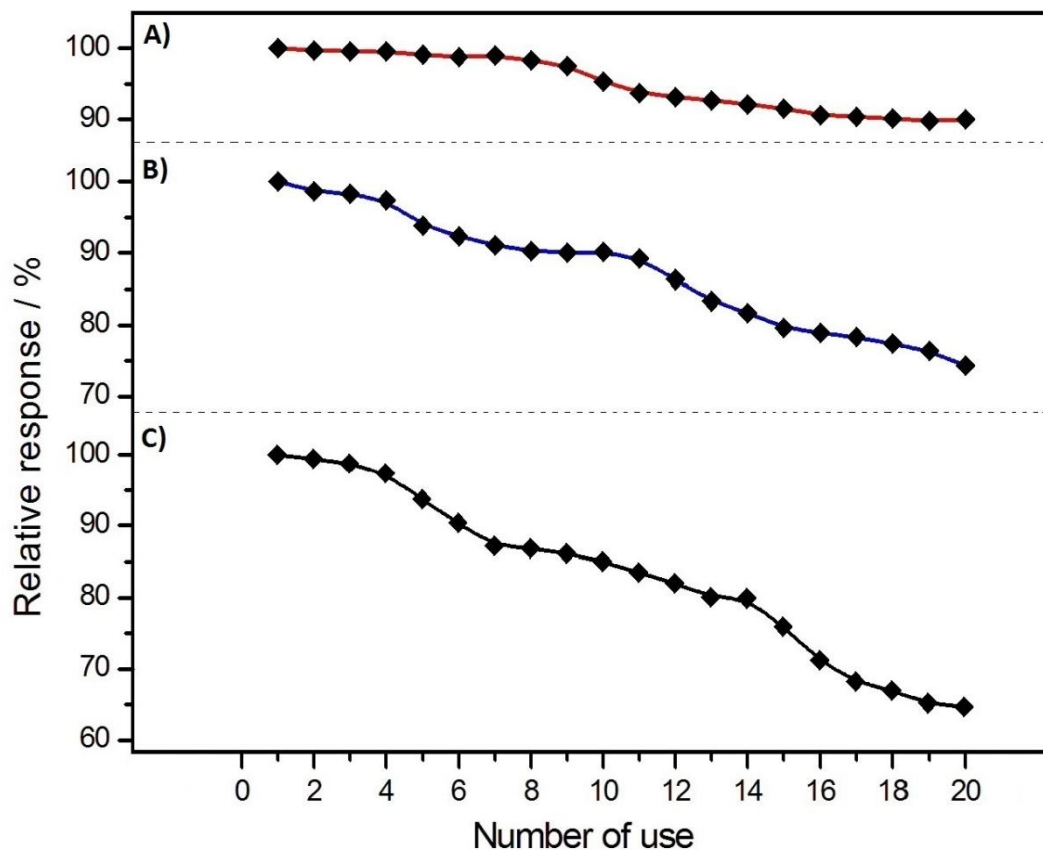


Figure 4.21 Operational stability of enzyme electrode A) P(Vfc<sub>0.4</sub>-GMA)/ REGO-Pt B), P(Vfc<sub>0.4</sub>-GMA)/ REGO-Pd and C) P(Vfc<sub>0.4</sub>-GMA)/ REGO-Au

Operation stability of biosensor represents important factor in enzyme electrode design. It was performed by 20 consequent measurements with single enzyme electrode in electrochemical cell with reference and counter electrode in 10mM PBS pH 7.00 at room temperature with applied potential of 0.35V and after each measurement electrode was stored for recovery at 4°C for 5 min. Amperometric current response of P(Vfc<sub>0.4</sub>-GMA)/ REGO-Pt electrode (see Figure 4.21 A) was stable in first 8 measurements after which it started gradually to decrease and eventually loses 10% of its initial response. P(Vfc<sub>0.4</sub>-GMA)/ REGO-Pd electrode (see Figure 4.21 B) showed stability in first four

measurements after which it slowly decreased for 30% and eventually retained 70% of its initial response, and finally P(Vfc<sub>0.4</sub>-GMA)/ REGO-Au electrode (see Figure 4.21 C) showed huge decrease in current response and retained its 60% of initial response. In the end, P(Vfc<sub>0.4</sub>-GMA)/ REGO-Pt fabricated enzyme retain 90% of initial response which might be explained by good interaction between enzyme and the polymer used as well as fast electron transfer and showed by that big reliability in xanthine detection.

#### 4.4.2 Storage Stability

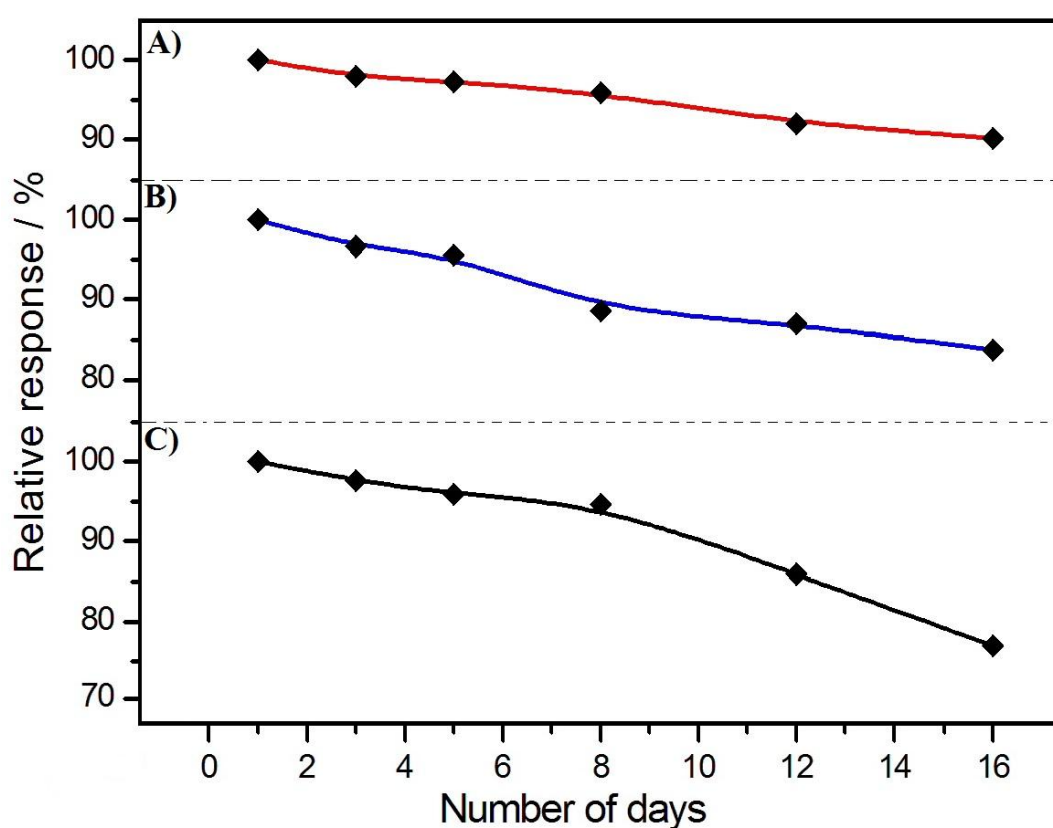


Figure 4.22 Storage stability of enzyme electrode A) P(Vfc<sub>0.4</sub>-GMA)/ REGO-Pt B), P(Vfc<sub>0.4</sub>-GMA)/ REGO-Pd and C) P(Vfc<sub>0.4</sub>-GMA)/ REGO-Au

Storage stability is important parameter of biosensors performance testing which needs to be investigated in order to see shelf life of the electrode and effect of storage on its response. Testing was performed by proposed electrodes in period of 16 days, in

which single electrode was used for xanthine detection after which was stored in 10mM PBS pH 7.0, 4°C. As it can be seen from results (see Figure 4.22), three different electrodes was used to perform this experiments. Electrode fabricated by P(Vfc<sub>0.4</sub>-GMA)/ REGO-Pt gave the most satisfying results by retaining 90% of its initial response after 16 days of storage (see Figure 4.22 A). Second electrode tested is based on P(Vfc<sub>0.4</sub>-GMA)/ REGO-Pd has small decrement of 5% in first 5 days after which current response decreases for 20% (see Figure 4.22 B) and in the end electrode based on P(Vfc<sub>0.4</sub>-GMA)/ REGO-Au retained 75 % of its initial amperometric response (see Figure 4.22 C). This reduction in current response of enzyme activity as a function of time maybe occurred because of denaturation of enzyme or some of the immobilized enzymes dropped from the electrode by the time. However, the electrode based P(Vfc<sub>0.4</sub>-GMA)/ REGO-Pt showed best results and relatively small amperometric current response of 10% when compared to other proposed electrodes.

#### 4.5 ANALYTICAL PERFORMANCE

Table 4.4 Analytical performance and efficiency in detection of Xanthine of proposed biosensors

Electrode	Xanthine added ( $\mu\text{M}$ )	Xanthine found ( $\mu\text{M}$ )	Erorr (%)
Poly(VFc <sub>0.4</sub> -GMA)/REGO-Au	5	5.12	2.4
	10	9.56	4.4
	15	14.78	1.46
Poly(VFc <sub>0.4</sub> -GMA)/REGO-Pd	5	4.78	4.4
	10	9.89	1.1
	15	14.67	2.2
Poly(VFc <sub>0.4</sub> -GMA)/REGO-Pt	5	4.95	1
	10	9.98	0.2
	15	15.1	0.66

Analytical performance and efficiency in detection of xanthine of biosensor was performed by addition of known xanthine concentration (see Table 4.4). Obtained current responses from each addition were calculated and interpreted using calibration curves (see Figure 4.20) and represented as error in percentages (%). As seen best results are obtained by P(Vfc<sub>0.4</sub>-GMA)/ REGO-Pt based biosensor which has error from

0.2 to maximum percentage 1% (out of 100%) which shows very big reliability and accuracy in xanthine detection. As well other proposed electrodes based on P(Vfc<sub>0.4</sub>-GMA)/ REGO-Pd and P(Vfc<sub>0.4</sub>-GMA)/ REGO-Au also showed high reliability in xanthine detection in which error is very low.

#### 4.6 INTERFERENCE

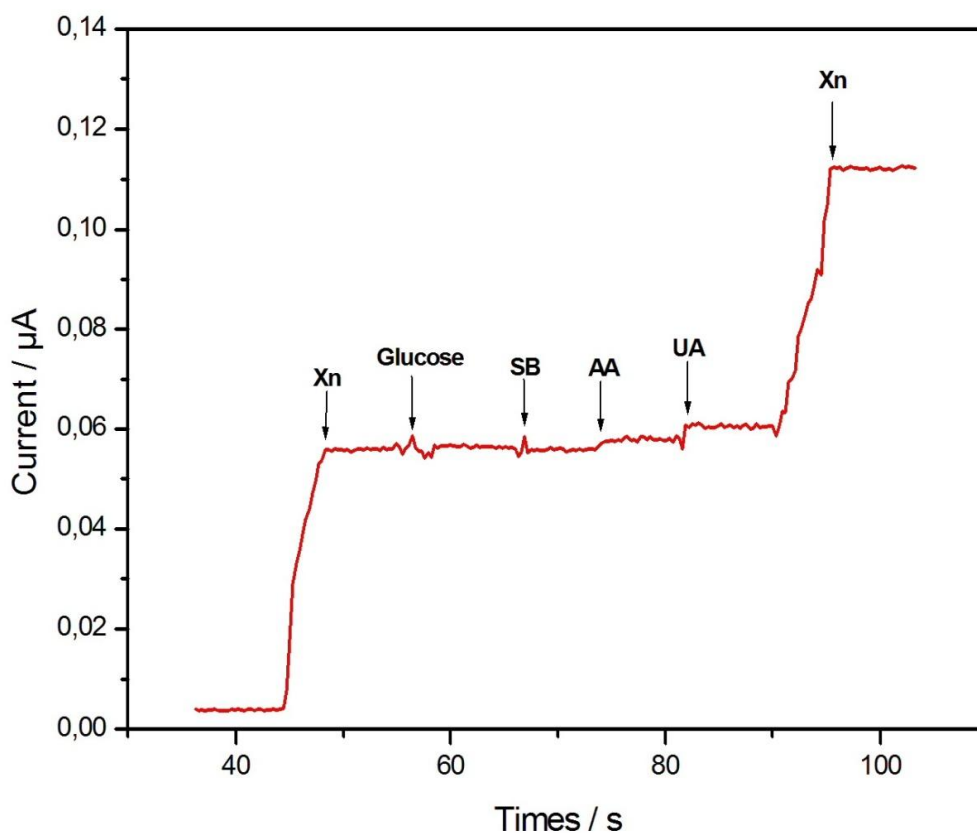


Figure 4.23 Interference effect of Glucose, Sodium Benzoate (SB), Ascorbic Acid (AA) and Uric Acid (UA) to the current response of Xanthine (Xn) in 10mM pH 7.0 PBS at applied potential of 0.35V with P(Vfc<sub>0.4</sub>-GMA)/ REGO-Pt proposed electrode

Interferents which probably might have impact on amperometric current response of proposed biosensor are glucose, ascorbic acid (AA), uric acid (UA) and sodium benzoate (SB). Electrode used for interference study has been selected by looking previous results obtained and it has been concluded that best candidate is P(Vfc<sub>0.4</sub>-GMA)/ REGO-Pt based electrode. As it can be seen from results (see Figure

4.23) there is no huge impact of interferences to enzyme electrode which was added between two 3 $\mu$ M additions of xanthine. Only substances which had some worth of mentioning effect are ascorbic acid (AA) and uric acid (UA) which was in total around 6% of total effect on current response. These small changes occurred when interferences are added might be contributed to low applied potential of 0.35V. It is well known that applied potentials for UA and AA are 0.75V and 0.55V (Matos et al., 2000) and as well it is confirmed in early studies (Dervisevic et al., 2015a) in which low applied potential is good enough to minimize interference to negligible level.

#### 4.7 REAL-SAMPLE APPLICATION

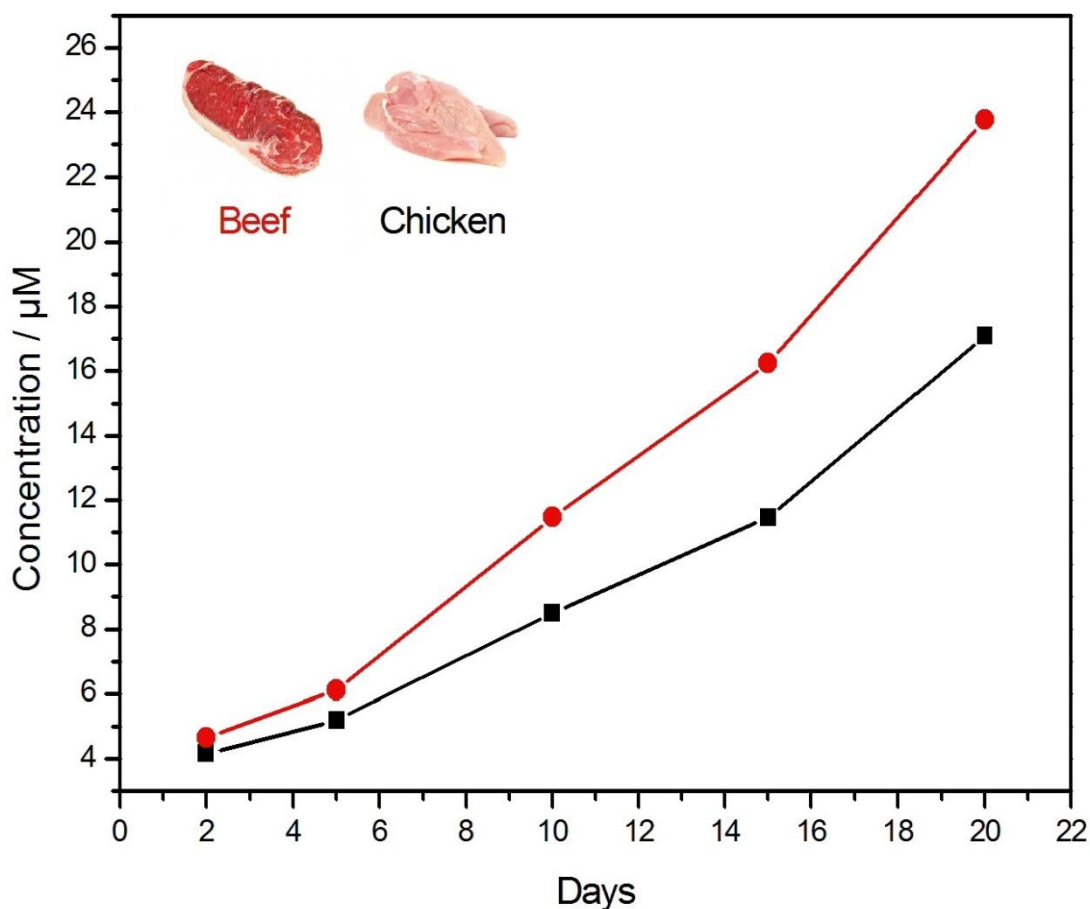


Figure 4.24 Determination of xanthine in beef and chicken meat samples using P(Vfc<sub>0.4</sub>-GMA)/ REGO-Pt fabricated electrode in 10mM PBS pH 7.0, applied potential 0.35V

Xanthine is one of the major metabolites of ATP degradation (see Figure 1.2) as well its concentration reflects meat freshness (Yano et al., 1995). Xanthine as an indicator of beef and chicken meat spoilage has been investigated using reliable and sensitive proposed P(Vfc<sub>0.4</sub>-GMA)/ REGO-Pt coated electrode. Meat freshness control has been performed by testing xanthine concentration in 2, 5, 10, 15 and 20 days old beef and chicken meat using P(Vfc<sub>0.4</sub>-GMA)/ REGO-Pt coated electrode. After the sample preparation (see section 3.9.) amount of xanthine concentration in it, has been tested by proposed biosensor and amperometric respond has been recorded respectively. Data was interpreted using previously obtained calibration curve (see Figure 4.20) and its optimized parameters which are linear range (1 to 40 µM) and detection limit

(0.003 $\mu$ M). Obtained results have been presented in terms of concentration vs. days of meat storage (see Figure 4.24). In the 2 days old meat xanthine concentration was nearly 4 $\mu$ M after which it was gradually increasing till 5<sup>th</sup> day where beef and chicken meat started to show different results (as expected) which in final beef xanthine concentration reached 24 $\mu$ M and chicken 17  $\mu$ M in 20<sup>th</sup> day of storage. It has to be noted that meats are purchased from local market and that values obtained are found to be in the scope of linear range. Final results have been supported by previous studies on xanthine detection reported in literature (Devi et al., 2013a, Dervisevic et al., 2015a, Dervisevic et al., 2015b).

## CHAPTER 5

### CONCLUSIONS

Amperometric xanthine biosensor has been successfully fabricated using REGO, REGO-Au, REGO-Pd and REGO-Pt and P(Vfc<sub>0.4</sub>-GMA) formed nanocomposites. Xanthine oxidase was covalently immobilized onto the nanocomposites film coated pencil graphite electrodes. During fabrication of biosensing surface, in order to ensure fast electron transfer ferrocene co-polymer was used as redox mediator between the immobilized XOD and the electrode surface and allowing low working potential. Low working potential is important especially in interference study since it helps to avoid some self oxidation molecules which can easily interfere in current response when high potential applied. The electrochemical amperometric response has been significantly improved by REGO, REGO-Au, REGO-Pd and REGO-Pt nanocomposites. However, electrode based on P(Vfc<sub>0.4</sub>-GMA)/ REGO-Pt nanocomposite only exhibit an excellent detection limit and wide linear range. Additionally biosensor showed excellent analytical performance in detection of xanthine with sensitivity of 21.98 $\mu$ A/  $\mu$ M , linear range 1 $\mu$ M to 40 $\mu$ M, fast response time of 2s and low detection limit 0.003 $\mu$ M (see Table 4.3.2), as such very reliable in xanthine detection and for that reason P(Vfc<sub>0.4</sub>-GMA)/ REGO-Pt coated electrode has been selected for interference and real sample measurements.

Electrode fabrications process includes synthesis of polymer and nano-materials after which these materials was successfully coated on electrode as a nanocomposite. During these processes material and surface characterization has been conducted in three parts, spectroscopic, electrochemical and morphological. Spectroscopic measurements such as FT-IR, RAMAN, UV and XRD analyses from

which detail study is conducted. Electrochemical measurements were composed of cyclic voltammogram (CV) and electrochemical impedance spectroscopy (EIS) in which coated electrodes electron transfer ability was studied in order to find optimum nanocomposite for xanthine biosensor application. Finally morphological study was performed using SEM and TEM analysis. After fabricated electrodes characterization has been completed, investigation continued in study of electrodes optimum working variables as analytical performance of electrode and shelf life.

In conclusion, amperometric biosensor has fabricated with excellent performance and very accurate detection of xanthine, making it very suitable method for meat freshness control. Advantage of this method is that it is very simple to use, there is no need for lab technicians, no need for long and complex procedures for sample preparation, as well expensive and massive equipment. Amperometric xanthine biosensor offers very fast, accurate and easy xanthine measurement, without complex procedures for sample preparation as well very simple application on site by ordinary works as well as very low cost. Additionally biosensor showed excellent analytical performance in detection of xanthine with sensitivity of  $21.98\mu\text{A}/\mu\text{M}$ , linear range  $1\mu\text{M}$  to  $40\mu\text{M}$ , fast response time of 2s and low detection limit  $0.003\mu\text{M}$  (see Table 4.3.2). Real sample application study has been conducted successfully and experimental data and results have been supported by the literature (Yano et al., 1995, Devi et al., 2013a, Dervisevic et al., 2015a).

## REFERENCES

- Abdulazeez, T.L., "Synthesis and utilisation of graphene for fabrication of electrochemical sensors", *Talanta*, Vol.131, pp. 424-443, 2015.
- Amine, A., Mohammadi, H., Bourais, I., Palleschi, G., "Enzyme inhibition-based biosensors for food safety and enviromental monitoring", *Biosensors and Bioelectronics*, Vol. 21, pp. 1405-1423, 2006.
- Banupriya, C., Ratnakar, Doureradjou, P., Mondal, N., Vishnu, B., Koner, B.C., "Can urinary excretion rate of malondialdehyde, uric acid and protein predict the severity and impending death in perinatal asphyxia" *Clinical Biochemistry*, Vol. 41, pp. 968–973, 2008.
- Beckman, J.S., Parks, D.A., Pearson, J.D., Marshall, P.A., Freeman, B.A., "A sensitive fluorometric assay for measuring xanthine dehydrogenase and oxidase in tissues" *Free Radical Biology and Medicine*, Vol. 6, pp. 607–615, 1989.
- Berti, G., Fossati, P., Tarenghi, G., Musitelli, C., Melzideril, G.V., "Enzymatic colorimetric method for the determination of inorganic phosphorus in serum and urine" *J. Chemical Clinical Biochemistry*, Vol. 26, pp. 399–404, 1988.
- Bong, G.C., Jinkyu, I., Hoon, S.K., HoSeok, P., "Flow-injection amperometric glucose biosensors based on graphene/Nafion hybrid electrodes", *Electrochimica Acta*, Vol. 56, pp. 9721–9726, 2011.
- Brandt, R.K., Hughes, M.R., Bourget, L.P., Truszkowska, K., and Greenler, R.G., "The interpretation of CO adsorbed on Pt/SiO<sub>2</sub> of two different particle-size distributions", *Surface Science*, Vol. 286, pp. 15–25, 1993.
- Campion, E.W., Glynn, R.J., Delabry, L.O., "Asymptomatic hyperuricemia. Risks and consequences in the Normative Aging Study", *American Journal of Medicine*, Vol. 82, pp. 421–426, 1987.
- Carsol, M.A., Volpe, G., Mascini, M., "Amperometric detection of uric acid and hypoxanthine with Xanthine oxidase immobilized and carbon based screen-printed electrode. Application for fish freshness determination", *Talanta*, Vol. 44, pp. 2151–2159, 1997.
- Chen, G., Chu, Q., Zhang, L., Ye, J., "Separation of six purine bases by capillary electrophoresis with electrochemical detection", *Analitica Chimica Acta*, Vol. 457 pp. 225–233, 2002.

- Caussé, E., Pradelles, A., Dirat, B., Negre-Salvayre, A., Salvayre, R., Couderc, F., “Simultaneous determination of allantoin, hypoxanthine, xanthine, and uric acid in serum/plasma by CE”, *Electrophoresis*, Vol. 28, pp. 381–387, 2007.
- Chabard, J.L., Lartigue-Mattei, C., Vedrine, F., Petit, J., Berger, J.A., “Mass fragmentographic determination of xanthine and hypoxanthine in biological fluids”, *Journal of Chromatography*, Vol. 221, pp. 9-17, 1980.
- Chao, J., Zhu, D., Zhang, Y., Wang, L., Fan, C., “DNA nanotechnology-enabled biosensors”, *Biosensors and Bioelectronics*, doi:10.1016/j.bios.2015.07.007, 2015.
- Chaubey, A., Malhotra, B.D., “Mediated biosensors”, *Biosensor and Bioelectronics*, Vol. 17, pp. 441-456, 2002.
- Clark, L.C. Jr., Lyons, C., “Electrode systems for continuous monitoring in cardiovascular surgery”, *Annals of New York Academy of Science*, Vol. 102, pp. 29-45, 1962.
- Cooper, N., Khosravan, R., Erdmann, C., Fiene, J., Lee, J.W., “Quantification of uric acid, xanthine and hypoxanthine in human serum by HPLC for pharmacodynamic studies”, *Journal Chromatogr B*, Vol. 837, pp. 1–10, 2006.
- Dervisevic, M., Custiuc, E., Cevik, E., Şenel, M., “Construction of novel xanthine biosensor by using polymeric mediator/MWCNT nanocomposite layer for fish freshness detection”, *Food Chemistry*, Vol. 181, pp. 277–283, 2015a.
- Devi, R., Thakur, M., Pundir, C.S., “Construction and application of an amperometric xanthine biosensor based on zinc oxide nanoparticles-polypyrrole composite film”, *Biosensors and Bioelectronics*, Vol. 26, pp. 3420–3426, 2011.
- Devi, R., Sandeep, Y., Renuka, N., Sujata, Y., Pundir, C.S., “Electrochemical biosensor based on gold coated iron nanoparticles/chitosan composite bound xanthine oxidase for detection of xanthine in fish meat”, *Journal of Food Engineering*, Vol. 115, pp. 2017-205, 2012a.
- Devi, R., Yadav, S., Pundir, C.S., “Amperometric determination of xanthine in fish meat by zinc oxide nanoparticle/chitosan/multiwalled carbon nanotube/polyaniline composite film bound xanthine oxidase”, *Analyst*, Vol. 137, pp. 754–759, 2012b.
- Devi, R., Batra, B., Lata, L., Yadav, S., Pundir, C.S., “A method for determination of xanthine in meat by amperometric biosensor based on silver nanoparticles/cysteine modified Au electrode”, *Process Biochemistry*, Vol. 48, pp. 242-249, 2013a.
- Devi, R., Yadav, S., Nehra, R., Yadav, S., Pundir, C.S., “Electrochemical biosensor based on gold coated iron nanoparticles/chitosan composite bound xanthine oxidase for detection of xanthine in fish meat”, *Journal of Food Engineering*, Vol. 115, pp. 207–214, 2013b.

- Dervisevic, M., Custiuc, E., Çevik, E., Durmus, Z., Şenel, M., Durmus, A., “Electrochemical biosensor based on REGO Fe<sub>3</sub>O<sub>4</sub> bionanocomposite interference for xanthine detection in fish sample”, *Food Control*, Vol. 57, pp. 402-410, 2015b.
- Durmus, Z., Durmus, A., Kavas, H., “Synthesis and characterization of structural and magnetic properties of graphene/hard ferrite nanocomposites as microwave-absorbing material”, *Journal of Materials Science*, Vol. 50, pp. 1201-1213, 2015.
- Dalkiran, B., Kaçar, C., Erden, P.E., Kilic, E., “Amperometric xanthine biosensors based on chitosan-Co<sub>3</sub>O<sub>4</sub>-multiwall carbon nanotube modified glassy carbon electrode”, *Sensors and Actuators B*, Vol. 200, pp. 83–91, 2014.
- Dimcheva, N., Horozova, E., Jordanova, Z., “An amperometric xanthine oxidase enzyme electrode based on hydrogen peroxide electroreduction”, *Zeitschrift für Naturforschung*, Vol. 57, pp. 883–889, 2002.
- Du, X.S., Xiao, M., Meng, Y.Z., Hay, A.S., “Novel synthesis of conductive poly(arylene disulfide)/graphite nanocomposite”, *Synthetic Metals*, Vol. 143, pp. 129–32, 2004.
- Eggins, B.R., "Sensing Elements" in Ando, D.J. (Eds.), *Chemical Sensors and Biosensors*, Wiley, pp. 69-106, United Kingdom, 2011.
- Frank, J., Kelleher, D. K., Pompella, A., Thews, O., Biesalski, H. K., Vaupel, P., “Enhancement of oxidative cell injury and antitumor effects of localized 44°C hyperthermia upon combination with respiratory hyperoxia and xanthine oxidase”, *Cancer Research*, Vol. 58, pp. 2693-2698, 1998.
- FAOSTAT, Food and Agriculture Organization of the United Nations (2014). Retrieved from: <http://faostat.fao.org/site/610/default.aspx#ancor>
- Feng, J.X., Zhang, Q.L., Wang, A.J., Wei, J., Chen, J.R., Feng, J.J., “Caffeine assisted facile synthesis of platinum@platinum core shell nanoparticles supported on reduced graphene oxide with enhanced electrocatalytic activity for methanol oxidation”, *Electrochimica Acta*, Vol. 142, pp. 343–350, 2014.
- Farnaz, L., Zohreh, S., Pooria, M., Yatimah, A., Ninie, S., “One-step hydrothermal green synthesis of silver nanoparticle-carbon nanotube reduced-graphene oxide composite and its application as hydrogen peroxide sensor”, *Sensors and Actuators B*, Vol. 208, pp. 389–98, 2015.
- Gerard, M., Chaubey, A., Malhorta, B.D., “Application of conducting polymers to biosensors”, *Biosensors and Bioelectronics*, Vol. 17, pp. 345-359, 2002.
- Horecker, B. L., Heppel, L.A., “Reduction by cytochrome c of xanthine oxidase”, *Journal of Biological Chemistry*, Vol. 178, pp. 683, 1949.
- Hummers, W.S., Offeman, R.E., “Preparation of Graphitic Oxide”, *Journal of American Chemical Society*, Vol. 80, pp. 1339-1339, 1958.

- Hiratsuka, A., Fujisawa, K., Muguruma, H., “Amperometric biosensor based on glucose dehydrogenase and plasma-polymerized thin films”, *Analytical Sciences*, Vol. 24, pp. 483-486, 2008.
- Hongmin, M., Dan, W., Zhentao, C., Yan, L., Yong, Z., Bin, D., Qin, W., “Graphene-based optical and electrochemical biosensors: A review”, *Analytical Letters*, Vol. 46, pp. 1–17, 2013.
- Kalimuthu, P., Leimkühler, S., Bernhardt, P.V., “Low-Potential Amperometric Enzyme Biosensor for Xanthine and Hypoxanthine”, *Analytical Chemistry*, Vol. 84, pp. 10359–10365, 2012.
- Kawachi, M., Kono, N., Mineo, I., Yamada, Y., Tarui, S., “Decreased xanthine oxidase activities and increased urinary oxypurines in heterozygotes for hereditary xanthiuria”, *Clinica Chimica Acta*, Vol. 188, pp. 137–146, 1990.
- Kim, K.Y., Schumacher, R.H., Hunsche, E., Wertheimer, A.I., Kong, S.X., “A literature review of epidemiology and treatment of acute gout”, *Clinical Therapeutics*, Vol. 25, pp. 1593–1617, 2003.
- Kock, R., Delvoux, B., Gresling, H., “A high-performance liquid chromatographic method for the determination of hypoxanthine, xanthine, uric acid and allantoin in serum.” *Journal of Clinical Chemistry and Clinical Biochemistry*, Vol. 31, pp. 303–310, 1993.
- Lawal, A.T., Adeloju, S.B., “Progress and recent advances in fabrication and utilization of hypoxanthine biosensors for meat and fish quality assessment: A review”, *Talanta*, Vol. 100, pp. 217–228, 2012a.
- Lawal, A.T., Adeloju, S.B., “Mediated xanthine oxidase potentiometric biosensors for hypoxanthine based on ferrocene carboxylic acid modified electrode”, *Food Chemistry*, Vol. 135, pp. 2982–2987, 2012b.
- Luong, J.H.T., Male, K.B., Nguyen, A.L., “Application of polarography for monitoring the fish post-mortem metabolite transformation”, *Enzyme Microbial Technology*, Vol. 11, pp. 277–282, 1989.
- Litwack, G., Bothwell, J.W., Williams, J.N., Elvehjem, C.A., “A colorimetric assay for xanthine oxidase in rat liver homogenates”, *Journal of Biological Chemistry*, Vol. 200, pp. 303–310, 1953.
- Li, Y., Hermann, J.S., Xu, S., “Gold nanoparticle-based biosensors”, *Gold Bulletin*, Vol. 43 pp. 29-41, 2010.
- Mello, L.D., Kubota, L.T., “Review of the use of biosensors as analytical tools in the food and drink industries”, *Food Chemistry*, Vol. 77 pp. 237–256, 2002.
- McMaster-Fay, R.A., “Pre-eclampsia: a disease of oxidative stress resulting from the catabolism of DNA (primarily fetal) to uric acid y xanthine oxidase in the maternal liver; a hypothesis”, *Bioscience Hypotheses*, Vol. 1, pp. 35–43, 2008.

- Mulchandani, A., Luong, J.T.H., Male, K.B., "Development and application of a biosensor for hypoxanthine in fish extract", *Analitica Chimica Acta*, Vol. 221, pp. 215-222, 1989.
- MacLeod, G., "The scientific and technological basis of meat flavours", in Birch, G.G. and Lindley, M.G. (Eds.), *Developments in Food Flavours*, Elsevier Applied Science: London, pp. 151-172, United Kingdom, 1986.
- Matos, R.C., Augelli, M.A., Lago, C.L., Angnes, L., "Flow injection analysis- amperometric determination of ascorbic and uric acids in urine using arrays of gold microelectrodes modified by electrodeposition of palladium", *Analytica Chimica Acta*, Vol. 404, pp. 151-157, 2000.
- McCreery, R.L., "Advanced carbon electrode materials for molecular electrochemistry", *Chemical Reviews*, Vol. 108, pp. 2646-87, 2008.
- Nychas, G.J.E., Skandamis, P.N., Tassou, C.C., Koutsoumanis, K.P., "Meat spoilage during distribution", *Meat Science*, Vol. 78, pp. 77-89, 2008.
- Nan-Fu, C., Teng-Yi, H., "Sensitivity and kinetic analysis of graphene oxide-based surface plasmon resonance biosensor", *Sensors and Actuator B: Chemica*, Vol. 197, pp. 35-42, 2014.
- Ono, T., Tsuruta, R., Fujita, M., Aki, H. S., Kutsuna, S., Kawamura, Y., Wakatsuki, J., Aoki, T., Kobayashi, C., Kasaoka, S., Maruyama, I., Yuasa, M., Maekawa, T., "Xanthine oxidase is one of the major sources of super oxide anion radicals in blood after reperfusion in rats with forebrain ischemia/reperfusion", *Brain Research*, Vol. 1305, pp. 158-167, 2009.
- Olojoa, R.O., Xiab, R.H., Abramsona, J.J., "Spectrophotometric and fluorometric assay of superoxide ion using 4-chloro-7-nitrobenzo-2-oxa-1, 3-diazole" *Analytical Biochemistry*, Vol. 339, pp. 338-344, 2005.
- Ostrovsky, P.M., Gornyi, I.V., Mirlin, A.D., "Electron transport in disordered graphene", *Physical Review B*, Vol. 74, pp. 235-443, 2006.
- Pereira, P.M.C.C., Vicente, A.F.R.B., "Meat nutritional composition and nutritive role in the human diet", *Meat Science*, Vol. 93, pp. 586-592, 2013.
- Parker, R., Snedden, W., Watts, R.W., "The mass-spectrometric identification of hypoxanthine and xanthine ('oxypurines') in skeletal muscle from two patients with congenital xanthine oxidase deficiency (xanthinuria)" *Biochemical Journal*, Vol. 115, pp. 103-108, 1969.
- Park, S., An, J., Potts, J.R., Velamakanni, A., Murali, S., Ruoff, R.S., "Hydrazine-reduction of graphite- and graphene oxide", *Carbon*, Vol. 49, pp. 3019-3023, 2011.
- Pei, J., Li, X.Y., "Xanthine and hypoxanthine oxidase sensors based on xanthine oxidase immobilized on a PuPtCl<sub>6</sub> chemically modified electrode and liquid chromatography electrochemical detection", *Analytical Chimica Acta*, Vol. 414, pp. 205-213, 2000.

- Peck, M.C.P., Marano, R.S., Schuetzle, D., Riley, T.L., Hampton, C.V., Prater, T.J., Skewes, L.M., Jensen, T.E., “Determination of Nitrated Polynuclear Aromatic Hydrocarbons in Particulate Extracts by Capillary Column Gas Chromatography with Nitrogen Selective Detection”, *Analytical Chemistry*, Vol. 55, pp. 1946-1954, 1983.
- Pumera, M., “Graphene-based nanomaterials and their electrochemistry”, *Chemical Society Reviews*, Vol. 39, pp. 4146–57, 2010.
- Rashed, M.S., Saadallah, A.A.A., Rahbeeni, Z., Eyaid W., Seidahmed, M.Z., Al-Shahwan, S., Salih, M.A.M., Osman, M.E., Al-Amoudi, M., Al-Ahaidib, L., Jacob, M., “Determination of urinary S-sulphocysteine, xanthine, and hypoxanthine by liquid chromatography–electrospray tandem mass spectrometry”, *Biomedical Chromatography*, Vol. 12, pp. 223–230, 2005.
- Renata, S., Pagliarussi, L., Luís, A.P., Freitas, L., Bastos, J.K., “A quantitative method for the analysis of xanthine alkaloids in Paullinia cupana (guarana) by capillary column gas chromatography”, *Journal of Separation Science*, Vol. 25, pp. 371–374, 2002.
- Sadeghi, S., Fooladi, E., Malekaneh, M., “A nanocomposite/crude extract enzyme-based xanthine biosensor”, *Analytical Biochemistry*, Vol. 464, pp. 51–59, 2014.
- Sassolas, A., Blum, L.J., Leca-Bouvier, B.D., “Immobilization strategies to develop enzymatic biosensors”, *Biotechnology Advances*, Vol. 30, pp. 489–511, 2012.
- Shang, N.G., Papakonstantinou, P., McMullan, M., Chu, M., Stamboulis, A., Potenza, A., Dhesi, S.S., Marchetto, H., “Catalyst-free efficient growth, orientation and biosensing properties of multilayer graphene nanoflake films with sharp edge planes”, *Advanced Functional Materials*, Vol. 18, pp. 3506–14, 2008.
- Tikk, M., Tikk, K., Torndren, M.A., Meinert, L., Aaslyng, M.D., Karlsson, A.H., Andersen, H.J., “Development of Inosine Monophosphate and Its Degradation Products during Aging of Pork of Different Qualities in Relation to Basic Taste and Retronasal Flavor Perception of the Meat”, *Journal of Agricultural and Food Chemistry*, Vol. 54, pp. 7769-7777, 2006.
- Tang, L., Wang, Y., Li, Y., Feng, H., Lu, J., Li, J., “Preparation, structure, and electrochemical properties of reduced graphene sheet films”, *Advanced Functional Materials*, Vol. 19, pp. 2782–2789, 2009.
- Taylor, R.F., Ingrid, G.M., Spencer, R.H., “Antibody- and receptor-based biosensors for detection and process control”, *Analytical Chimica Acta*, Vol. 249, pp. 67-70, 1991.
- Urdike, S.J., Hicks, G.P., “The enzyme electrode”, *Nature*, Vol. 214, pp. 986-988, 1967.
- Yano, Y., Kataho, N., Watanabe, M., Nakamura, T., Asano, Y., “Evaluation of beef aging by determination of hypoxanthine and xanthine contents: application of a xanthine sensor”, *Food Chemistry*, Vol. 52, pp. 439-445, 1995.

- Yoo, E.H., Lee, S.Y., “Glucose biosensors: An overview of use in clinical practice”, *Sensor*, Vol. 10, pp. 4558-4576, 2010.
- Yang, W., Ratinac, K.R., Ringer, S.P., Thordarson, P., Gooding, J.J., Braet, F., “Carbon nanomaterials in biosensors: Should you use nanotubes or graphene”, *Angewadte Chemie International Edition*, Vol. 49, pp. 2114–38, 2010.
- Zhigang, Z., Luis, G.G., Andrew, J.F., Huaqing, X., Francis, M., William, I.M., “A Critical Review of Glucose Biosensors Based on Carbon Nanomaterials: Carbon Nanotubes and Graphene”, *Sensors*, Vol 12, pp. 5996-6022, 2012.
- Zengjie, F., Qianqian, L., Peiwei, G., Bin, L., Jinqing, W., Shengrong, Y., “A new enzymatic immobilization carrier based on graphene capsule for hydrogen peroxide biosensors”, *Electrochimica Acta*, Vol. 151, pp. 186–94, 2015.
- Zhao, Z.,H. Jiang., “Enzyme-based Electrochemical Biosensors”, in Serra P.A. (Ed.), *Biosensor*, pp. 302, InTech, 2010.